

# Chapter 2

## Vibrations of Lumped-Parameter Systems

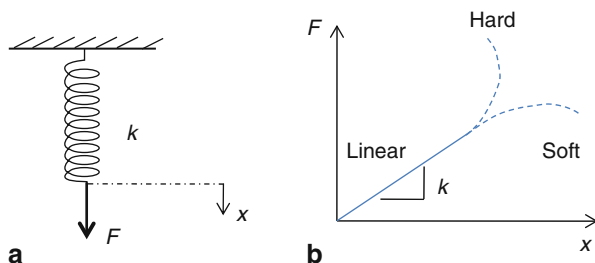
This chapter presents an overview and a refresher on the linear vibration principles of lumped-parameters systems, which are used to model MEMS. Since most microstructures undergo some sort of vibratory motion, the information presented here are fundamental to the understanding of many key aspects of MEMS dynamical behavior. Also, some of the methods to extract the parameters needed to model MEMS devices and structures require knowledge in the principles of vibrations. In addition, this chapter serves as a good introduction to the more advanced topics of nonlinear oscillations that will be discussed in the following chapters. The principles of operation of some MEMS devices, including accelerometers, gyroscopes, and band-pass filters, will be discussed here.

In lumped-parameters systems, MEMS devices are modeled as lumped or concentrated masses, springs, dampers, and point forces. The discussion will start on single-degree-of-freedom (SDOF) systems. The free vibration problem (damped and undamped) will be discussed. Then, forced vibrations due to external point loads and due to base excitations will be addressed. Arbitrary excitation will be also discussed. Finally, the analysis of the vibration of two-degree-of-freedom (2-DOF) systems will be presented. For more in-depth treatment of these topics, the readers are referred to these excellent references in vibrations [1–5].

### 2.1 Introduction

Vibration can be defined as the study of repetitive motion of objects relative to a stationary frame [1]. There are many examples of vibrations in our everyday life, such as heart beating, cars vibrations on bumpy roads, and the motion of tree branches with wind. In MEMS, most devices employ a microstructure or more that is either driven intentionally to vibrate to achieve sensing or actuation functions, such as microresonators and atomic force microscopes (AFM), or they undergo some sort of vibratory motion when excited by dynamic disturbances, such as when microstructures are subjected to mechanical shock.

**Fig. 2.1** **a** A schematic shows a spring being pulled by a force. **b** A force–deflection curve showing a linear regime with a slope  $k$  ending with a possible nonlinear hardening or softening behaviors



For vibration to occur there must be an exchange of energy between potential and kinetic energy. Hence, a vibratory system must have a spring-like component that stores the potential energy and converts it to kinetic energy in the form of motion. Complaint structures, such as beams and rods, play the role of springs in MEMS. If the spring is loaded with a force, Fig. 2.1a, and its deflection is measured then a force–displacement curve can be generated, such as that of Fig. 2.1b. Typically, the curve is a straight line for small range of force (linear range). The slope of this line is a constant called the stiffness coefficient of the spring  $k$ . Beyond the linear regime, the spring shows a nonlinear force–deflection relationship characterized by either increasing in stiffness (hardening behavior) or decreasing in stiffness (softening behavior) compared to the linear case.

To describe the motion of a system undergoing vibrations, a number of independent coordinates need to be assigned to the system to adequately describe its motion. These are called degrees of freedom (DOFs). For example, a body that undergoes translational and rotational motion in a single plane requires two independent variables to describe its motion, one for translation and one for rotation (unless both are related). If the vibration is induced by initially disturbing the system from its equilibrium position without having a force that continuously acting on it, the vibration is called free vibration (vibration due to initial conditions). If a force acts continuously on the system during motion, the vibration is called forced vibration. Vibration also can be classified as damped or undamped depending on whether the energy of the system is conserved or is being dissipated during vibration. Next, we discuss some of these types of vibrations.

## 2.2 Free Vibration of Single-Degree-of-Freedom Systems

### 2.2.1 Undamped Vibration

Many systems that have one mode of motion dominating their response or one principal DOF can be modeled as SDOF systems. In the absence of damping or dissipation mechanisms, a lumped spring–mass system, such as that of Fig. 2.2a, can be used to represent this system. The first step in the vibration analysis is the dynamics, that

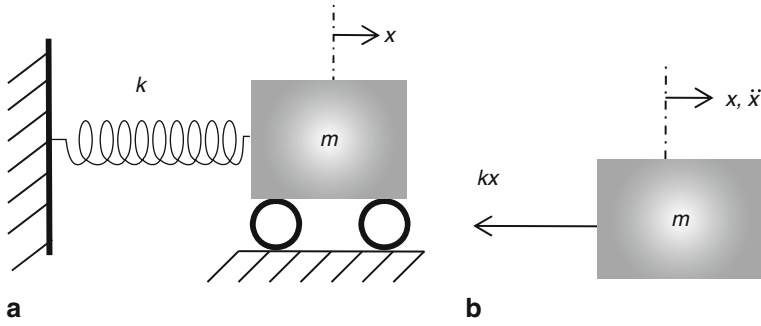


**Fig. 2.2** **a** A spring–mass system to model the free vibration of a conservative SDOF system. **b** A diagram showing the forces acting on the mass in the horizontal direction when disturbed to the positive direction to the right

is, we need first to derive the equation of motion for the system. For this, Newton’s second law of motion is used:

$$\sum \vec{F} = m\vec{a} \quad (2.1)$$

where  $\sum \vec{F}$  represents the forces acting on the mass  $m$  in a specific direction and  $\vec{a}$  is the induced acceleration of the mass in that direction. To apply Eq. (2.1) on the system, the mass is assumed displaced in the positive direction (to the right) a distance  $x$ . Then, we isolate the mass, label all the forces acting on it, and label the acceleration  $\vec{a}$  in the positive direction, which is the same as that of  $x$  as shown in Fig. 2.2b. We recall here that the acceleration  $\vec{a}$  is the second-time derivative of the displacement,  $\vec{a} = \ddot{x}$ , where the superscript dot denotes a time derivative. As noted from Fig. 2.2b, when the mass is displaced to the right, there will be a resistance restoring force acting on it to the left, which assuming a linear relationship as in Fig. 2.1b is expressed as

$$\vec{F} = -kx \quad (2.2)$$

where the negative sign in Eq. (2.2) indicates that the force has an opposite direction to the positive displacement to the right. Applying Eq. (2.1) yields

$$-kx = m\ddot{x} \quad (2.3)$$

or after rearranging

$$m\ddot{x} + kx = 0. \quad (2.4)$$

Dividing Eq. (2.4) by  $m$  gives

$$\ddot{x} + \omega_n^2 x = 0 \quad (2.5)$$

where  $\omega_n^2 = k/m$  and  $\omega_n$  is called the natural frequency of the system. It has the unit of rad/s. It depends on the “natural” characteristics of the system, mass and stiffness. Equation (2.5) represents a second-order linear differential equation of constant coefficients. To solve this equation, we assume  $x$  to be of the form

$$x(t) = ae^{\lambda t} \quad (2.6)$$

where  $t$  is the time,  $a$  and  $\lambda$  are unknown constants, and  $e$  is the exponential constant. Substituting Eq. (2.6) into Eq. (2.5) and dividing by  $ae^{\lambda t}$  yields the following characteristic equation for  $\lambda$ :

$$\lambda^2 + \omega_n^2 = 0. \quad (2.7)$$

From Eq. (2.7),  $\lambda^2 = \pm i\omega_n$ , and hence according to Eq. (2.6) and using the principle of superposition, the total solution of Eq. (2.5) becomes

$$x(t) = a_1 e^{i\omega_n t} + a_2 e^{-i\omega_n t} \quad (2.8)$$

where  $a_1$  and  $a_2$  are the constants of integration that are determined from the initial conditions of the system (its initial velocity and displacement). Alternatively, using Euler’s formulas, Eq. (2.8) can be written as

$$x(t) = A \sin(\omega_n t + \phi) \quad (2.9)$$

where  $A$  and  $\phi$  are the constants of integration. Equation (2.9) describes the oscillatory motion of the system of Fig. 2.2a over time with  $A$  representing the amplitude of oscillation and  $\phi$  the phase shift. To determine  $A$  and  $\phi$ , we assume the system has an initial velocity  $v_0$  and an initial displacement  $x_0$ , that is

$$x(0) = x_0; \quad \dot{x}(0) = v_0. \quad (2.10)$$

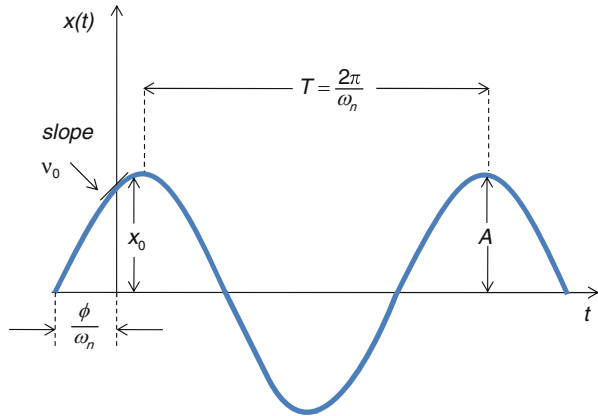
From Eqs. (2.9) and (2.10)

$$A = \sqrt{x_0^2 + (v_0/\omega_n)^2}; \quad \phi = \tan^{-1}(\omega_n x_0/v_0). \quad (2.11)$$

Figure 2.3 shows an example plot of Eq. (2.9) clarifying the terminologies defined above. As seen in the figure, the resulting motion is an oscillatory motion that repeats itself every time interval  $T$ . This time is called the natural period. It is related to the natural frequency by  $T = 2\pi/\omega_n$  and has the unit of time. As noted, the natural period indicates how “frequent” the motion repeats itself in one cycle  $T$ . The inverse of  $T$ ,  $f$ , is also called the natural frequency and it has the unit of (1/s) or Hertz (Hz). Hence,

$$f = \frac{1}{T} = \frac{\omega_n}{2\pi}. \quad (2.12)$$

**Fig. 2.3** A portion of the time–history response of the spring–mass system of Fig. 2.2a indicating some of the key vibration features of the system. In the figure,  $x_0 > 0$  and  $v_0 > 0$



To obtain the mass velocity and acceleration, Eq. (2.9) is derived with respect to time once and twice, respectively, which yields

$$\dot{x}(t) = \omega_n A \cos(\omega_n t + \phi) \quad (2.13)$$

$$\ddot{x}(t) = -\omega_n^2 A \sin(\omega_n t + \phi). \quad (2.14)$$

One can note from Eq. (2.13) that the magnitude of the maximum velocity is  $\omega_n A$  with a phase shift  $\pi/2$  with respect to the displacement. Also from Eq. (2.14), the magnitude of the maximum acceleration is  $\omega_n^2 A$  with a phase shift  $\pi$  with respect to the displacement and  $\pi/2$  with respect to the velocity.

**Example 2.1:** A system operates in vacuum, as in the case of some MEMS resonators, can be modeled as an undamped spring–mass system, such as that of Fig. 2.2. In an experiment to determine the mass and stiffness of the system, its natural frequency was measured and found to be 100 Hz. Then, a new mass was added to the system equals 1 g and the natural frequency was measured again and found to be 90 Hz. Determine the stiffness and mass of this system.

**Solution:** Given:  $f_1 = 100$  Hz,  $f_2 = 90$  Hz,  $\delta m = 0.001$  kg.  
From Eq. (2.12)

$$f_1 = \frac{\omega_1}{2\pi} = \frac{\sqrt{k/m}}{2\pi} \quad (a)$$

$$f_2 = \frac{\omega_2}{2\pi} = \frac{\sqrt{k/(m + \delta m)}}{2\pi}. \quad (b)$$

Dividing Eq. (a) over Eq. (b)

$$\frac{f_1}{f_2} = \frac{\sqrt{k/m}}{\sqrt{k/(m + \delta m)}} = \sqrt{\frac{m + \delta m}{m}}. \quad (c)$$

Squaring Eq. (c)

$$\left(\frac{f_1}{f_2}\right)^2 = \frac{m + \delta m}{m}. \quad (d)$$

Solving for  $m$  gives

$$m = \delta m \frac{f_2^2}{f_1^2 - f_2^2}. \quad (e)$$

Substituting the numbers yields  $m = 4.3$  g. Solving for  $k$  from Eq. (a) gives  $k = 1.683$  kN/m.

## 2.2.2 Damped Vibration

The model presented in Sect. 2.2.1 predicts an oscillatory motion that keeps going forever and never dies out. A more realistic model of vibrating systems should account for the fact that the energy of vibrations dissipates over time through damping mechanisms. One way to account for this is by adding a dashpot or a damper element to the model of Fig. 2.2a. If the damping force  $\vec{F}_d$  is assumed linearly proportional to the speed of the mass, as in the case of viscous damping from air, then the damping force can be expressed as

$$\vec{F}_d = -c\dot{x} \quad (2.15)$$

where  $c$  is the viscous damping coefficient and the minus sign indicates that the force is a resistance force with a direction opposite to the motion direction. It should be noted here that MEMS damping mechanisms can be more complicated and may be nonlinear, as will be discussed in the next chapter. Figure 2.4 shows a schematic for the model and the corresponding force diagram.

Applying Newton's second law on the system of Fig. 2.4 yields the below equation of motion:

$$m\ddot{x} + c\dot{x} + kx = 0. \quad (2.16)$$

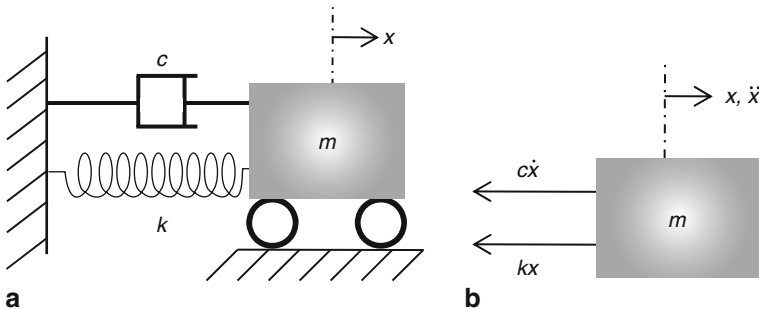


**Fig. 2.4** **a** A spring–mass–damper system to model the free vibration of a nonconservative SDOF system. **b** A diagram showing the forces acting on the mass in the horizontal direction when disturbed to the positive direction to the right

Dividing Eq. (2.16) by  $m$  yields

$$\ddot{x} + 2\zeta\omega_n\dot{x} + \omega_n^2x = 0 \tag{2.17}$$

where  $\zeta$  is called the damping ratio, a nondimensional quantity, defined as

$$\zeta = \frac{c}{2m\omega_n}. \tag{2.18}$$

To solve Eq. (2.17), we substitute Eq. (2.6) into Eq. (2.17) and divide the outcome by  $ae^{\lambda t}$  to yield

$$\lambda^2 + 2\zeta\omega_n\lambda + \omega_n^2 = 0. \tag{2.19}$$

Solving Eq. (2.19) gives

$$\lambda_{1,2} = -\zeta\omega_n \pm \omega_n\sqrt{\zeta^2 - 1} \tag{2.20}$$

and hence using the principle of superposition, the total solution of Eq. (2.17) is

$$x(t) = a_1e^{\lambda_1 t} + a_2e^{\lambda_2 t}. \tag{2.21}$$

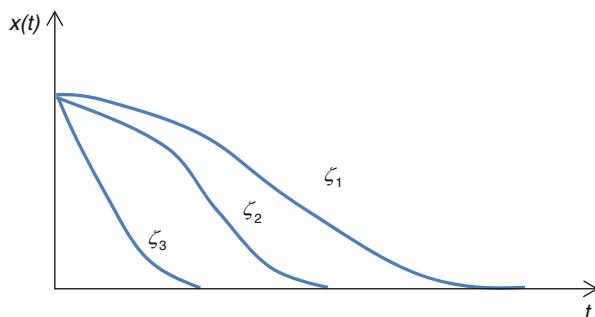
As noted from Eqs. (2.20) and (2.21), the nature of the response depends on whether  $\lambda_1$  and  $\lambda_2$  are complex, real, or mix. This in turn depends on the square-root term in Eq. (2.20) and particularly whether  $\zeta$  is less than one, greater than one, or equal one. Accordingly, the free vibration of damped systems can be classified into the following categories:

1. Overdamped motion ( $\zeta > 1$ )

As the name suggests, this case indicates too much damping. In this case,  $\lambda_1$  and  $\lambda_2$  are pure real numbers. Hence, the solution of the system can be expressed as

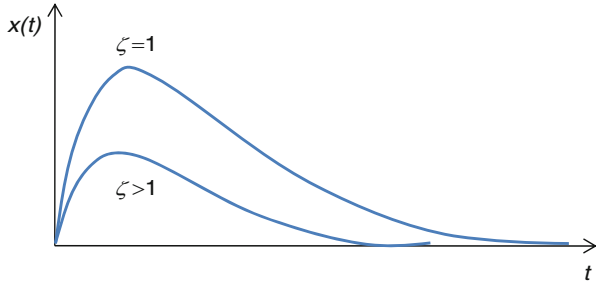
$$x(t) = e^{-\zeta\omega_n t} \left[ a_1e^{\omega_n t\sqrt{\zeta^2-1}} + a_2e^{-\omega_n t\sqrt{\zeta^2-1}} \right]. \tag{2.22}$$

Figure 2.5 shows a plot of the response of Eq. (2.22) for various damping ratios. As seen in the figure, the response in this case is not oscillatory; the damping is too



**Fig. 2.5** Examples of time-history responses of an overdamped spring-mass-damper system for various damping ratios for  $1 < \zeta_1 < \zeta_2 < \zeta_3$ . In the figure,  $x_0 > 0$  and  $v_0 = 0$

**Fig. 2.6** A comparison for the response of a spring–mass–damper system between the critically damped and overdamped cases. In the figure,  $x_0 = 0$  and  $v_0 > 0$



much that the motion dies very quickly without allowing for oscillations. The rate of motion decaying increases with the amount of damping and the value of  $\zeta$ .

### 2. Critically damped motion ( $\zeta = 1$ )

This case is called “critically” damped because it separates two different qualitative behaviors: oscillatory motion for  $\zeta < 1$  and non-oscillatory motion for  $\zeta > 1$ . In this case, Eq. (2.20) gives two real equal roots,  $\lambda_{1,2} = -\omega_n$ . Hence, the solution of Eq. (2.17) becomes

$$x(t) = e^{-\omega_n t}(a_1 + a_2 t). \quad (2.23)$$

The response of the system in this case is similar to the overdamped case except that decaying of the motion takes longer time. Figure 2.6 compares the response of this case to an overdamped case.

### 3. Underdamped motion ( $0 < \zeta < 1$ )

As the name suggests, this case indicates low damping compared to the other two cases. Here,  $\lambda_1$  and  $\lambda_2$  are complex numbers. To remind ourselves of this,  $\lambda_1$  and  $\lambda_2$  are rewritten from Eq. (2.20) explicitly with the imaginary root  $i$ , that is

$$\lambda_{1,2} = -\zeta\omega_n \pm i\omega_n\sqrt{1-\zeta^2}. \quad (2.24)$$

Hence, the solution for the system motion according to Eq. (2.21) becomes

$$x(t) = e^{-\zeta\omega_n t} \left[ a_1 e^{i\omega_n t\sqrt{1-\zeta^2}} + a_2 e^{-i\omega_n t\sqrt{1-\zeta^2}} \right]. \quad (2.25)$$

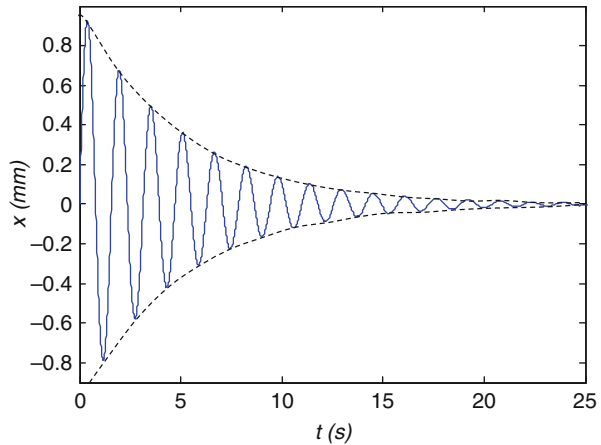
Using Euler’s formula, Eq. (2.25) can be rewritten in the more convenient form as

$$x(t) = A e^{-\zeta\omega_n t} \sin[\omega_d t + \phi] \quad (2.26)$$

where  $A$  and  $\phi$  are the amplitude and phase of the response, respectively and  $\omega_d = \omega_n\sqrt{1-\zeta^2}$  is the damped natural frequency of the system. In the case of low values of  $\zeta$ ,  $\omega_d \approx \omega_n$ . The parameters  $A$  and  $\phi$  are determined from the initial conditions of the system. Using Eqs. (2.10) and (2.26) yields

$$\tan(\phi) = \frac{x_0\omega_d}{v_0 + \zeta x_0\omega_n}; \quad A = \frac{\sqrt{(x_0\omega_d)^2 + (v_0 + \zeta x_0\omega_n)^2}}{\omega_d} \quad (2.27)$$

**Fig. 2.7** An example of a time–history response of an underdamped spring–mass–damper system. In the figure,  $x_0 = 0$  and  $v_0 > 0$



An example of the response obtained from Eq. (2.26) is plotted in Fig. 2.7. The figure shows an oscillatory motion that decays exponentially with time (note the exponential envelope in dashed lines). As noted from Figs. 2.5, 2.6, and 2.7, underdamped motion is the only damped case that can be considered as “true” vibration motion where the moving mass passes through the equilibrium position more than once. Also, underdamped motion is the most common; hence, the majority of vibration analysis and studies are focused on this case.

Before closing this section, we should point out to the fact that in all of the above discussion, we implicitly assumed that the damping ratio  $\zeta$  or the damping coefficient  $c$  to be positive. If otherwise damping is negative then the resulting motion will be unstable vibratory motion (flutter), which usually leads to the collapse or failure of the structure (a famous example of this case is the collapse of the Tacoma Bridge in 1940). A similar note applies on the stiffness  $k$ , which must be positive also. In short, both the stiffness and damping of the system must be positive to lead to stable vibration. More on stability issues are discussed in Chap. 5.

**Example 2.2:** A spring–mass–damper system, Fig. 2.4, has  $m = 1$  kg,  $k = 100$  N/m, and  $c = 1$  kg/s. If the system is given an initial velocity of 10 mm/s while it is in the equilibrium position, determine and plot the response of the system. If the system vibrates, determine the frequency of vibration due to this excitation in Hz.

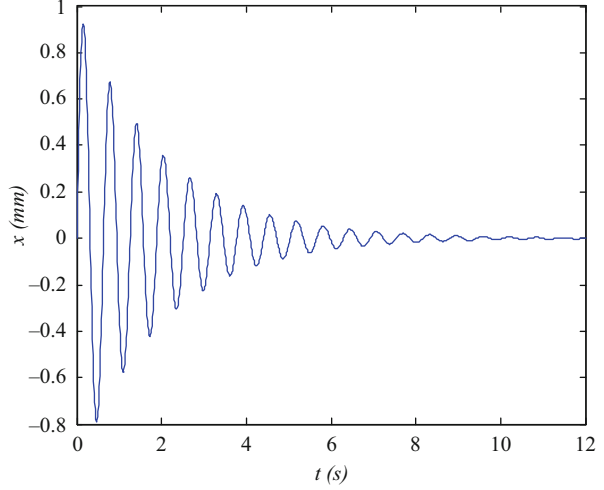
**Solution:** First, the system needs to be determined if it is overdamped, underdamped, or critically damped. Hence, we need to calculate  $\zeta$ , but first we calculate  $\omega_n$

$$\omega_n = \sqrt{\frac{k}{m}} = \sqrt{\frac{100}{1}} = 10 \text{ rad/s.} \quad (\text{a})$$

From Eq. (2.18)

$$\zeta = \frac{c}{2m\omega_n} = \frac{1}{2(1)(10)} = 0.05. \quad (\text{b})$$

**Fig. 2.8** A time–history response of the underdamped system of Example 2.2



Hence, the system is underdamped. It vibrates with  $\omega_d$  given by

$$\omega_d = \omega_n \sqrt{1 - \zeta^2} = 10 \sqrt{1 - .05^2} = 9.9875 \text{ rad/s} \quad (c)$$

and in Hz

$$f = \frac{\omega_d}{2\pi} = 1.59 \text{ Hz.} \quad (d)$$

As can be seen, for low damping,  $\omega_n$  and  $\omega_d$  are almost the same. However, this tiny difference can be translated to hundreds of Hz for microstructures with mega- and gigahertz frequencies.

To determine the response,  $A$  and  $\phi$  are calculated from Eq. (2.27)

$$\tan(\phi) = \frac{x_0 \omega_d}{v_0 + \zeta x_0 \omega_n} = \frac{0 \times \omega_d}{v_0 + \zeta x_0 \omega_n} = 0 \Rightarrow \phi = 0 \text{ rad.} \quad (e)$$

$$A = \frac{\sqrt{(x_0 \omega_d)^2 + (v_0 + \zeta x_0 \omega_n)^2}}{\omega_d} = \frac{\sqrt{(0)^2 + (.01 + 0)^2}}{9.9875} = 0.001 \text{ m.} \quad (f)$$

Hence, from Eq. (2.26), the response of the system is expressed as

$$x(t) = .001 e^{-.5t} \sin[9.9875t]. \quad (g)$$

Figure 2.8 shows a plot of the response.

### 2.3 Forced Harmonic Excitation of Single-Degree-of-Freedom Systems

Harmonic excitation is very common in MEMS through actuation methods, such as electrostatic and piezoelectric actuation. In this section, the forced vibration of a SDOF system, Fig. 2.9a, to a harmonic force excitation is analyzed. From

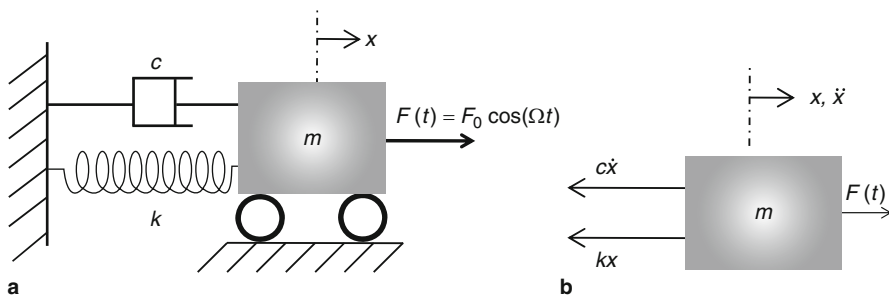


**Fig. 2.9** **a** A model for the forced vibration of a spring–mass–damper system. **b** A diagram showing the forces acting on the mass in the horizontal direction when disturbed to the positive direction to the right

the force diagram of Fig. 2.9b, the equation of motion of the system can be written as

$$m\ddot{x} + c\dot{x} + kx = F_0 \cos(\Omega t) \quad (2.28)$$

where  $F_0$  is the harmonic force amplitude and  $\Omega$  is the excitation frequency. Dividing Eq. (2.28) by  $m$  yields

$$\ddot{x} + 2\zeta\omega_n\dot{x} + \omega_n^2x = f_0 \cos(\Omega t) \quad (2.29)$$

where  $f_0 = F_0/m$ . Equation (2.29) is a nonhomogenous linear differential equation of constant coefficients. Hence, its solution consists of two parts: a homogenous solution  $x_h$  and a particular solution  $x_p$ . The homogenous solution corresponds to the case when  $f_0 = 0$ , which is similar to the cases discussed in Sect. 2.2. Thus, depending on the damping ratio,  $x_h$  can be calculated by either of Eqs. (2.9), (2.22), (2.23), or (2.26). However, the constant of integrations cannot be calculated based on any of the formulas of Sect. 2.2; they need to be calculated based on relating the initial conditions to the total homogenous and particular solution of the system  $x = x_p + x_h$ . The homogenous solution represents physically the transient behavior of the system; hence, it decays away leaving only the particular solution, which is also called the steady-state response. To calculate the particular solution, the method of undetermined coefficients is used. Toward this,  $x_p$  is expressed as

$$x_p(t) = A_s \cos(\Omega t) + B_s \sin(\Omega t) \quad (2.30)$$

where  $A_s$  and  $B_s$  are unknown coefficients to be determined. Substituting Eq. (2.30) into Eq. (2.29) and solving for  $A_s$  and  $B_s$  (see [1] for details) yield

$$A_s = \frac{(\omega_n^2 - \Omega^2)f_0}{(\omega_n^2 - \Omega^2)^2 + 4\zeta^2\omega_n^2\Omega^2}; \quad B_s = \frac{2\zeta\omega_n\Omega f_0}{(\omega_n^2 - \Omega^2)^2 + 4\zeta^2\omega_n^2\Omega^2}. \quad (2.31)$$

A more convenient way to express this solution is through writing it in the form of an amplitude  $X$  and a phase  $\theta$  as

$$x_p(t) = X \cos(\Omega t - \theta) \quad (2.32)$$

where

$$X = \frac{f_0}{\sqrt{(\omega_n^2 - \Omega^2)^2 + (2\zeta\omega_n\Omega)^2}} \quad (2.33)$$

$$\theta = \tan^{-1} \left( \frac{2\zeta\omega_n\Omega}{\omega_n^2 - \Omega^2} \right). \quad (2.34)$$

If the forcing function in Eq. (2.28) is of the form  $F_0 \sin(\Omega t)$ , then the cosine is replaced with sine in Eq. (2.32), whereas Eq. (2.33) and Eq. (2.34) still apply. Equation (2.32) indicates an important fact for linear systems, that is if the system is excited with a frequency  $\Omega$ , it responds with the same frequency.

For convenience, the excitation frequency is normalized with respect to the natural frequency. This is a more meaningful way to describe the excitation frequency as a ratio of the natural frequency than just saying it as an absolute number, which does not reveal much unless it is known how far it is from the natural frequency. Thus, a normalized frequency ratio is introduced as  $r = \Omega/\omega_n$ . Accordingly, Eqs. (2.33) and (2.34) are rewritten as

$$\frac{X}{f_0/\omega_n^2} = \frac{1}{\sqrt{(1 - r^2)^2 + (2\zeta r)^2}} \quad (2.35)$$

$$\theta = \tan^{-1} \left( \frac{2\zeta r}{1 - r^2} \right). \quad (2.36)$$

Note that the ratio  $X/(f_0/\omega_n^2)$  is the dynamic steady-state response due to the harmonic force normalized to the static deflection of the system due to an equivalent static force of the same magnitude as the harmonic force (note that  $f_0/\omega_n^2 = F_0/m\omega_n^2 = F_0/k = \delta$ , where  $\delta$  is a constant). Therefore, this ratio indicates how much the response of the system is being amplified due to the dynamic effect. Note also that both sides of Eq. (2.35) are nondimensional.

Mostly in forced-vibration problems, the interest is in the steady-state response. In this case, Eq. (2.35) and (2.36) play key rule in revealing the vibration features of the system. Figures 2.10, 2.11, and 2.12 show plots of these equations while varying the damping ratio and the normalized excitation frequency. The following notes can be observed from Fig. 2.10:

- All the curves start from  $X/k = 1$ , which corresponds to very low excitation frequencies compared to the natural frequency. This range of excitation is called quasi-static. It is a stiffness-dominated range with slight effect from damping or inertia. By exciting the system near this range, one can extract the stiffness coefficient of the system if the amplitude of vibration is measured.
- The normalized response of all the curves become small and approach zero as  $r$  increases beyond  $r = 2$ . This range is called inertia-dominated range with slight effect from damping or stiffness. For sensor applications in MEMS, this range is not of much benefit since the system responds very weakly to the input excitation.

**Fig. 2.10** Frequency–response curves of spring–mass–damper system showing the normalized steady-state amplitude versus the normalized excitation frequency for various values of damping ratio

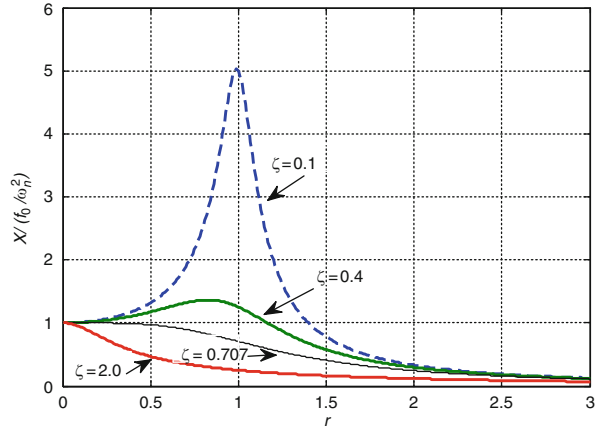
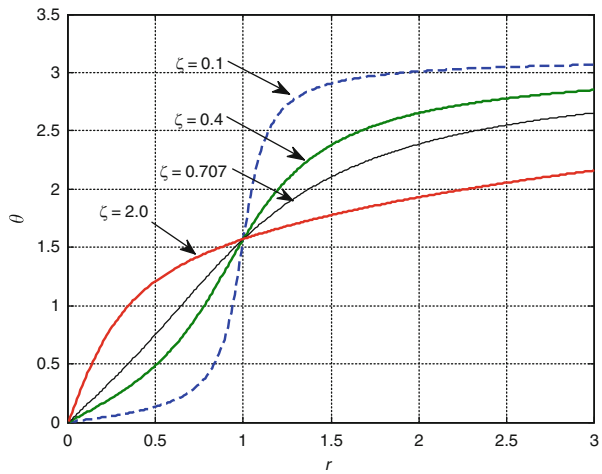
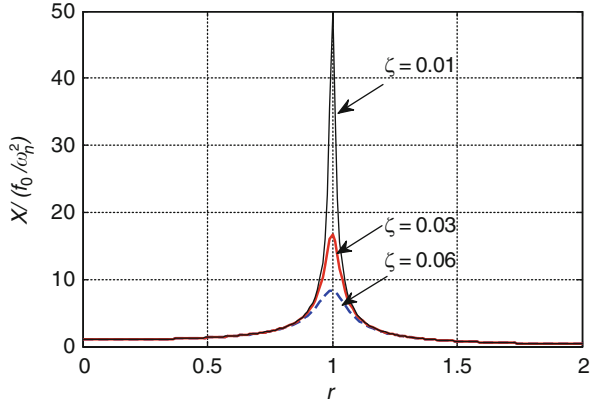


**Fig. 2.11** The phase angle of a spring–mass–damper system versus the normalized excitation frequency for various values of damping ratio



- For the range near  $0.5 < r < 1.5$ , the curves of small  $\zeta$  (0.4 and 0.1) peak in their value near  $r = 1$ . This corresponds to the so-called **resonance** phenomenon. It occurs when the excitation frequency is equal to the natural frequency and results in the maximum response for systems of low damping. Resonance is very important concept in vibration and MEMS as well. On the other hand, the curves of large  $\zeta$  (0.707 and 2) do not show any peak in their response. It turns out that all the curves of  $\zeta < 0.707$  have peak amplitudes somewhere close to  $r = 1$  whereas all the curves of  $\zeta > 0.707$  do not have any peaks. Because this range of  $r$  is very sensitive to damping, it is called damping dominated.
- While resonance most often corresponds to the maximum response of the system, it is not always the case, especially for large damping. In fact one can see that the maximum response for  $\zeta = 0.4$  is shifted slightly to the left. In general, the

**Fig. 2.12** Frequency–response curves for smaller values of the damping ratio



frequency corresponding to the peak response  $\Omega_{\text{peak}}$  is given by

$$\Omega_{\text{peak}} = \omega_n \sqrt{1 - 2\zeta^2}. \quad (2.37)$$

For small values of  $\zeta$ , the peak, resonance, and natural frequencies are almost the same.

From Fig. 2.11, the following can be noted:

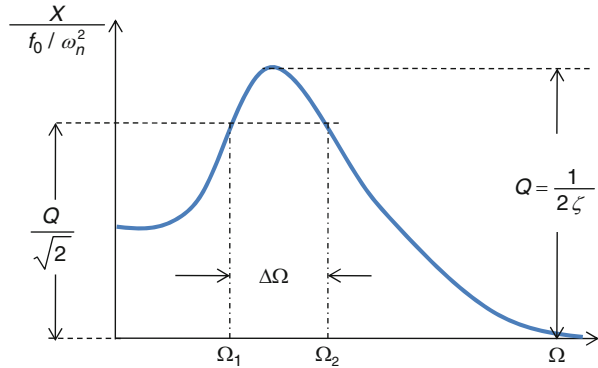
- All the curves pass through  $\theta = \pi/2$  at  $r = 1$ . This represents another indication of resonance corresponding to  $\pi/2$  phase shift.
- For values of  $r \ll 1$ ,  $\theta \approx 0$ . This means that for very small excitation frequencies, the response is almost in phase with the excitation force.
- For values of  $r \gg 1$ ,  $\theta \approx \pi$ . This means that for large excitation frequencies, the response is  $180^\circ$  out of phase with the excitation force.

Figure 2.12 shows frequency–response curves for small values of  $\zeta$ . Many MEMS resonators and sensors are operated in such conditions with even lower values of damping ratios. As seen in the figure, the curves become very sharp and narrow near resonance. In sensors, the interest is to achieve the highest response to give strong signal as an indication of what is being measured. The sharpness of resonance is commonly expressed in terms of a quantity called the quality factor  $Q$ , which is related to the damping ratio by

$$Q = \frac{1}{2\zeta}. \quad (2.38)$$

A rough estimation for the quality factor can be taken from the height of the resonance peak, as shown in Fig. 2.13. Another quantity of interest for sensors applications is the width of the resonance spike. As noted from Fig. 2.12, it is very hard to operate a resonator at the exact location of resonance for very small values of  $\zeta$ . Therefore, it is desirable to have the width of the spike as large as possible. A standard way to measure this width is through a quantity called bandwidth  $\Delta\Omega$ . To calculate the bandwidth, a

**Fig. 2.13** A frequency–response curve illustrating the concepts of quality factor and bandwidth



horizontal line is drawn intersecting with the frequency–response curve at a height of  $Q/\sqrt{2}$  as shown in Fig. 2.13. The height  $Q/\sqrt{2}$  represents the vibration amplitude that corresponds to half the maximum power (power is proportional to the amplitude squared). In decibel, this height represents  $-3$  dB. The points of intersection, called half-power points, are labeled  $\Omega_1$  and  $\Omega_2$ . The bandwidth is then expressed as [2]

$$\Delta\Omega = \Omega_2 - \Omega_1 = 2\zeta\omega_n. \tag{2.39}$$

Hence, from Eq. (2.38) and Eq. (2.39)

$$Q = \frac{\omega_n}{\Delta\Omega}. \tag{2.40}$$

Equation (2.40) is used to measure the quality factor, which more accurate than depending on measuring the height of the resonance peak. Equation (2.40) indicates that achieving high quality factor is on the expense of a good bandwidth and vice versa. This poses a challenge for MEMS and sensors applications. One way to overcome this and to achieve both high-quality factor and wide bandwidth is through using band-pass filters as sensors, as will be explained in Sect. 2.9.

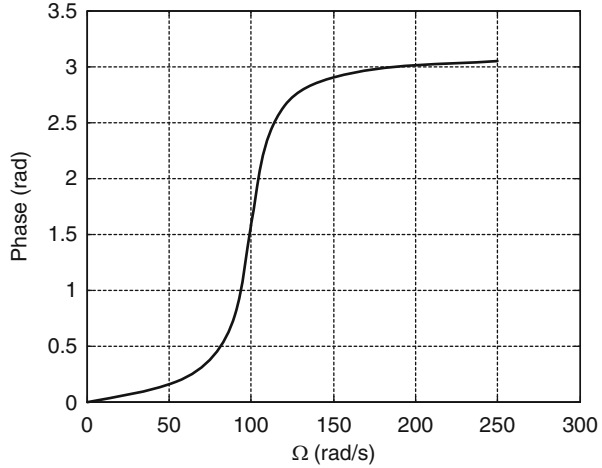
**Example 2.3:** Figure 2.14 shows the measured phase angle of the steady-state response of the system of Fig. 2.9a for a harmonic force of various excitation frequencies. If the system is then driven by  $F(t) = 200\cos(10t)$ , calculate the steady-state amplitude of the system assuming  $m = 1$  kg.

**Solution:** Based on Fig. 2.14, we note that the response has a phase shift  $\pi/2$  when  $\Omega = 100$  rad/s. This indicates resonance, which means that the natural frequency of the system is also 100 rad/s. Since the excitation frequency is given to be 10 rad/s, this means that  $r = 10/100 = 0.1$ . Hence, this is a quasi-static excitation case, in which knowing the damping is not important. According to Fig. 2.10, in this case

$$\frac{X}{f_0/\omega_n^2} \approx 1. \tag{a}$$

Accordingly,  $f_0 = F_0/m = 200$  N/kg and from (a)  $X \approx 0.02$  m.

**Fig. 2.14** A measured phase response for the system of Example 2.3



**Example 2.4:** Calculate the maximum response of the system of Example 2.2 if it is driven by a harmonic force of amplitude 10 N.

**Solution:** We recall from Example 2.4 that  $\omega_n = 10$  rad/s,  $\zeta = 0.05$ . Since the system is lightly damped, its maximum response occurs at resonance when  $r = 1$ . From Eq. (2.35)

$$\frac{X}{f_0/\omega_n^2} = \frac{1}{2\zeta}. \quad (\text{a})$$

Substituting  $f_0 = F_0/m = 10$  N/kg yields

$$\frac{X}{10/10^2} = \frac{1}{2(.05)} \Rightarrow X = 1 \text{ m}. \quad (\text{b})$$

## 2.4 Vibrating MEMS Gyroscopes

As an application for the previous section, we study here the vibration response of MEMS gyroscopes. A gyroscope is a device that captures the rotational motion of a body. More specifically, it is a device that measures the angular velocity of a body about a certain axis of rotation. Gyroscopes have wide range of uses in vehicle control applications, such as anti-rollover and antiskid control systems, aviation, navigation, space applications, robotics, and military applications, such as for missiles navigation. Conventional gyroscopes rely on large structures, such as tuning forks or spinning disks that are free to rotate in specific directions. Also, they may contain complicated components, such as bearings and rotating rings. Hence, the classical gyroscopes are bulky, expensive, and unreliable.

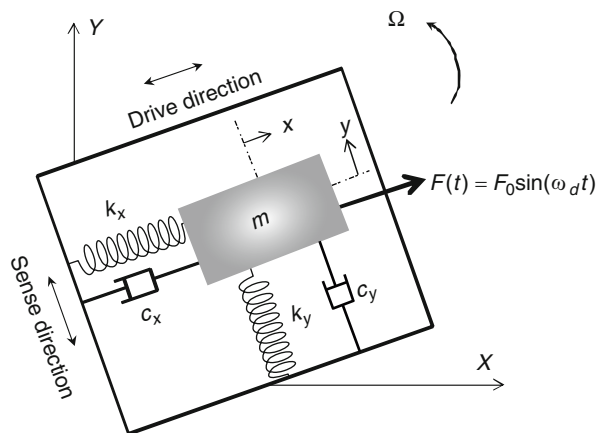
The technology of MEMS with the advantages of batch fabrication, small size, and low price has offered an attractive alternative to conventional gyroscopes. Almost all MEMS gyroscopes rely on vibrating mechanical elements that are driven to oscillate in the plane of the chip and to respond to rotation by another vibratory motion also in the same plane. This simple motion in a single plane and the fact that MEMS gyroscopes do not require complicated rotating parts or bearings have led to simplified and compact designs that can be easily fabricated using micromachining techniques.

MEMS gyroscopes have enabled smart generations of new technologies and applications, especially in consumer electronics, which would not have been possible before. MEMS gyroscopes are currently being used in video and still cameras and other portable electronics to help in the stabilization of their performance and to reduce the effect of human body motion and shaking. In addition, they are being used for interactive video games and head-mounted displays to sense and guide rotational motions.

The main principle of MEMS gyroscopes is the transfer of energy between two modes of vibrations, the drive and the sense modes, through the so-called Coriolis acceleration. Coriolis acceleration is an apparent acceleration that arises in a rotating frame and is proportional to the rate of rotation. The proof mass of MEMS gyroscopes can be driven and sensed using many methods; however, the most common is through electrostatic transduction. A major challenge in MEMS gyroscope is the fact that the generated Coriolis acceleration is very small. Hence, it is challenging to fabricate a small gyroscope of small mass with high sensitivity. More information on MEMS gyroscopes can be found in [6–8]. Next, we demonstrate through an example the basic dynamical and vibration features of a typical MEMS gyroscope.

**Example 2.5:** Consider the model of a vibratory MEMS gyroscope of Fig. 2.15. Derive the equations of motion of the device. Then, solve for the response of the

**Fig. 2.15** A model of a typical MEMS vibratory gyroscope



device when undergoing a rotational motion and derive an analytical expression for the device's sensitivity.

**Solution:** To derive the equations of motion, we need to apply Newton's second law, which requires determining the acceleration of the mass. The acceleration can be determined by taking twice the derivative of the position vector of the mass with respect to time as measured from a stationary frame of reference (the  $X$ - $Y$  frame in Fig. 2.15). An additional frame (the  $x$ - $y$  frame in Fig. 2.15) is also introduced, which rotates with the plane of the vibrating mass with an angular velocity  $\Omega$ . Both the stationary and rotating frames are assumed to share the same origin. The position vector  $\vec{R}$  of the mass can be written in terms of the  $x$ - $y$  frame as

$$\vec{R} = x\hat{b}_1 + y\hat{b}_2 \quad (\text{a})$$

where  $\hat{b}_1$  and  $\hat{b}_2$  are the unit vectors along the  $x$  and  $y$  coordinates, respectively. To find the velocity of the mass, the position vector is derived using the role of the time derivative of a rotating vector [9], which is

$$\frac{{}^{x-y}d\vec{R}}{dt} = \frac{{}^{x-y}d\vec{R}}{dt} + {}^{x-y}\vec{\omega} \times \vec{R} \quad (\text{b})$$

where  $\frac{{}^{x-y}d\vec{R}}{dt}$  refers to the time derivative of the vector with respect to the inertial frame,  $\frac{{}^{x-y}d\vec{R}}{dt}$  is the local derivative of the vector with respect to the rotating frame,  ${}^{x-y}\vec{\omega}$  is the rotational speed of the rotating frame (here assumed equal  $\Omega\hat{b}_3$ ), and  $\times$  refers to the cross product operation. Applying Eq. (b) on Eq. (a) yields the velocity vector  $\vec{V}$ :

$$\vec{V} = \dot{x}\hat{b}_1 + \dot{y}\hat{b}_2 + \Omega\hat{b}_3 \times (x\hat{b}_1 + y\hat{b}_2) \Rightarrow \vec{V} = (\dot{x} - \Omega y)\hat{b}_1 + (\dot{y} + \Omega x)\hat{b}_2. \quad (\text{c})$$

Similarly, taking one more time derivative of the velocity vector of Eq. (c) while applying the derivative role of Eq. (b) yields the acceleration vector  $\vec{a}$

$$\vec{a} = (\ddot{x} - \dot{\Omega}y - 2\dot{y}\Omega - \Omega^2x)\hat{b}_1 + (\ddot{y} + \dot{\Omega}x + 2\dot{x}\Omega - \Omega^2y)\hat{b}_2 \quad (\text{d})$$

where  $\dot{\Omega}$  is the angular acceleration. One can also arrive to Eq. (d) by applying directly the five-term acceleration formula for rotating frames [9].

Based on Eq. (d), and by considering the forces on the mass of Fig. 2.15, the equations of motion of the mass in the  $x$  and  $y$  directions can be written, respectively, as

$$-k_x x - c_x \dot{x} + F_0 \sin(\omega_d t) = m(\ddot{x} - \dot{\Omega}y - 2\dot{y}\Omega - \Omega^2x) \quad (\text{e})$$

$$-k_y y - c_y \dot{y} = m(\ddot{y} + \dot{\Omega}x + 2\dot{x}\Omega - \Omega^2y) \quad (\text{f})$$

where  $F_0$  and  $\omega_d$  are the driving force amplitude and frequency, respectively. Equations (e) and (f) represent two coupled differential equations. The coupling comes from the terms involving  $\dot{\Omega}$  and the two terms with "2" ( $2\dot{y}\Omega$  and  $2\dot{x}\Omega$ ), which are

nothing but the Coriolis acceleration terms. Equations (e) and (f) can be simplified by assuming constant angular speed, hence  $\dot{\Omega} = 0$ . Also, since  $\Omega$  is usually much smaller than the natural frequencies of the system, the terms involving  $\Omega^2$  can be dropped. Further, because the sense mode response  $y$  is much smaller than the response of the directly-excited drive mode  $x$ , the term  $2\dot{y}\Omega$  can be dropped. Under these simplifications, Eqs. (e) and (f) are reduced to

$$m\ddot{x} + k_x x + c_x \dot{x} = F_0 \sin(\omega_d t) \quad (g)$$

$$m\ddot{y} + k_y y + c_y \dot{y} = -2m\Omega \dot{x}. \quad (h)$$

Equation (g) can be solved independently of Eq. (h). Then the solution is substituted into Eq. (h), which is then solved for the sense-mode response  $y$ . To proceed, Eq. (g) is divided by  $m$ , hence it becomes

$$\ddot{x} + 2\zeta_x \omega_x \dot{x} + \omega_x^2 x = f_x \sin(\omega_d t) \quad (i)$$

where  $\omega_x = \sqrt{k_x/m}$ ,  $\zeta_x = c_x/(2m\omega_x)$ , and  $f_x = F_0/m$ . The solution of Eq. (i) is given by

$$x(t) = X \sin(\omega_d t - \phi) \quad (j)$$

where

$$X = \frac{f_x/\omega_x^2}{\sqrt{(1-r_x^2)^2 + (2\zeta_x r_x)^2}}; \quad \phi = \tan^{-1} \left( \frac{2\zeta_x r_x}{1-r_x^2} \right) \quad (k)$$

and  $r_x = \omega_d/\omega_x$ . To find the sense-mode response, Eq. (j) is substituted into Eq. (h), which after dividing by  $m$  becomes

$$\ddot{y} + \omega_y^2 y + 2\zeta_y \omega_y \dot{y} = f_y \cos(\omega_d t - \phi) \quad (l)$$

where  $\omega_y = \sqrt{k_y/m}$ ,  $\zeta_y = c_y/(2m\omega_y)$ , and  $f_y = -2\Omega\omega_d X$ . Hence, the amplitude of the sense-mode response can be written as

$$Y = \frac{f_y/\omega_y^2}{\sqrt{(1-r_y^2)^2 + (2\zeta_y r_y)^2}} = \left( \frac{2m\Omega\omega_d X}{k_y} \right) \frac{1}{\sqrt{(1-r_y^2)^2 + (2\zeta_y r_y)^2}} \quad (m)$$

where  $r_y = \omega_d/\omega_y$ . The sensitivity of the gyroscope is defined as the induced sense-mode amplitude (output) divided to the rotational speed (input), that is

$$\frac{Y}{\Omega} = \left( \frac{2m\omega_d X}{k_y} \right) \frac{1}{\sqrt{(1-r_y^2)^2 + (2\zeta_y r_y)^2}}. \quad (n)$$

One can see from Eq. (n) that the sensitivity is proportional to the oscillating mass, which puts some restrictions on the level of miniaturization that can be achieved

for MEMS gyroscopes. To achieve the highest sensitivity,  $X$  needs to be as large as possible. Hence, the mass usually is driven at resonance,  $r_x = 1$ . Also, resonance in the sense mode,  $r_y = 1$ , maximizes the sensitivity. This means that for maximum sensitivity  $\omega_d = \omega_y = \omega_x$ . Hence, substituting  $r_x = 1$  in Eq. (k) and then substituting the outcome and  $r_y = 1$  into Eq. (n) yield the below simplified expression for the sensitivity

$$\frac{Y}{\Omega} = \frac{2m\omega_d F_0 Q_x Q_y}{k_x k_y} \quad (o)$$

where  $Q_x = 1/2\zeta_x$  and  $Q_y = 1/2\zeta_y$  are the quality factors of the drive and sense modes, respectively. It is clear that high-quality factors are desirable to improve sensitivity.

Due to fabrication imperfections and environmental effects, it is extremely difficult to fabricate a gyroscope with  $\omega_y = \omega_x$  and to lock the driving frequency exactly at resonance. This is known as the frequency mismatch problem in the literature [6–8]. Adding more DOFs to the design of MEMS gyroscopes can alleviate this problem [8].

## 2.5 Base Excitations of SDOF Systems and Accelerometers Principles

Base excitation, also called support excitation, refers to the case when a structure or a device is placed on top of a moving floor with some damping and stiffness characteristics, such as isolation rubber floors. Also, it models the case when a structure is supported through elastic mounts, which can act as springs and dampers, such as shock absorbers in cars. When the floor or the supports move, they cause vibration to the structure, which is influenced by the stiffness and damping properties of the floor or the supports.

The above description refers to the classical scenarios for base excitation. In MEMS, base excitation represents a more common case. Flexible structures of MEMS in handheld devices and machinery components are excited into vibration through their supports. Essentially, any MEMS chip that contains a flexible structure will base-excite that structure if the chip is placed in an application where it moves. The flexibility of the structure plays the role of a spring, which is actuated from the base. MEMS accelerometers, gyroscopes, and pressure sensors inside a car are subjected to base excitation whenever the car hits a bump or even undergoes slight vibration. Accelerometers, including MEMS type, are intentionally designed to detect the motion properties of a moving base or a structure. In addition, several kinds of AFM rely on exciting a cantilever beam from its support, such as the tapping mode AFM.

Currently, there is considerable interest in harvesting energy from environmental vibrations. This can be done by designing flexible structures to be mounted over

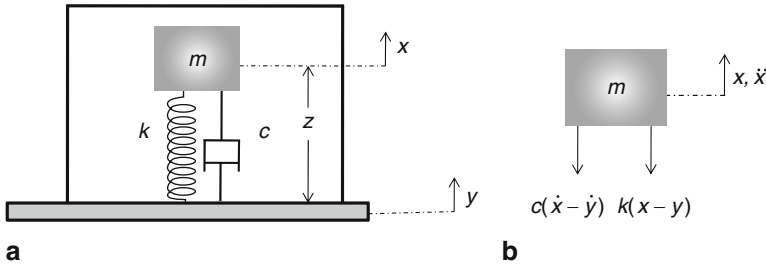


**Fig. 2.16** **a** A packaged device modeled as a spring–mass–damper system subjected to base excitation. **b** A diagram showing the forces acting on the mass when disturbed to the positive direction upward

a floor or a machine that undergoes slight vibration, for example a microwave or a dishwasher, such that the structures will be base-excited to vibration. Then the kinetic energy of the excited structures is converted into electricity through piezoelectric, electrostatic, or electromagnetic mechanisms [10, 11].

Figure 2.16a shows a schematic for a packaged device, for example an accelerometer, containing a flexible structure placed over a base that moves with displacement  $y(t)$ . Figure 2.16b shows a free-body diagram for the mass indicating the forces acting on it when displaced from its equilibrium position upward. Note here that the gravitational force of the weight is not included since it affects only the equilibrium position with no influence on the dynamic response (this is true for linear systems only). Based on Fig. 2.16b, the equation of motion of the mass can be written as

$$m\ddot{x} + k(x - y) + c(\dot{x} - \dot{y}) = 0 \quad (2.41)$$

where  $x$  is the absolute deflection of the mass. In MEMS applications, usually the structure is suspended a small distance above the substrate. Hence, an excessive support excitation can lead to a contact between the structure and the substrate, which may lead to the device failure. Thus, it is important to monitor the relative deflection  $z(t)$  of the structure with respect to the moving base, which is expressed as  $z = y - x$ . In addition, transduction mechanisms, such as electrostatic and piezoelectric, depend on this relative deflection. Writing Eq. (2.41) in terms of  $z$  yields

$$m\ddot{z} + c\dot{z} + kz = -m\ddot{y}. \quad (2.42)$$

The base is assumed to have harmonic excitation in the form of

$$y = Y \cos(\Omega_b t) \quad (2.43)$$

where  $Y$  denotes the amplitude of the base excitation and  $\Omega_b$  is its frequency. Substituting Eq. (2.43) into Eq. (2.42) and dividing the outcome by  $m$  yields

$$\ddot{z} + 2\zeta\omega_n\dot{z} + \omega_n^2 z = \Omega_b^2 Y \cos(\Omega_b t). \quad (2.44)$$

Equation (2.44) looks similar to Eq. (2.29) with  $f_0 = \Omega_b^2 Y$ . Defining  $r = \Omega_b/\omega_n$  and using Eqs. (2.35) and (2.36) result in the below expression for the steady state relative response:

$$z(t) = Z \cos(\Omega_b t - \theta) \quad (2.45)$$

where

$$\frac{Z}{Y} = \frac{r^2}{\sqrt{(1-r^2)^2 + (2\zeta r)^2}} \quad (2.46)$$

and  $\theta$  is as defined in Eq. (2.36).

The nondimensional ratio  $Z/Y$  represents an amplification factor indicating how much relative displacement is induced in the structure compared to the input displacement. Figure 2.17 shows a plot for  $Z/Y$  based on Eq. (2.46) for various damping ratios. It is observed that at resonance, the relative displacement reaches a maximum value for damping ratios below 0.707. For small values of  $r$ ,  $Z/Y$  is very small. It is noted also that all the curves converge to  $Z/Y \approx 1$  as  $r$  exceeds 3. Based on this interesting observation, the device shown in Fig. 2.16 can be used to measure the displacement of the base by relating it directly to the relative displacement of the mass, which can be transformed into a voltage signal for instance through piezoelectric, magnetic, or electrostatic methods. This is again provided that  $r > 3$ , which means that the natural frequency of the device should be at least below one-third of that of the frequency being measured. This implies that the device and its moving mass should be bulky and large to satisfy this requirement, which puts practical limitations on the use of such devices. This kind of measurement devices is called seismometer.

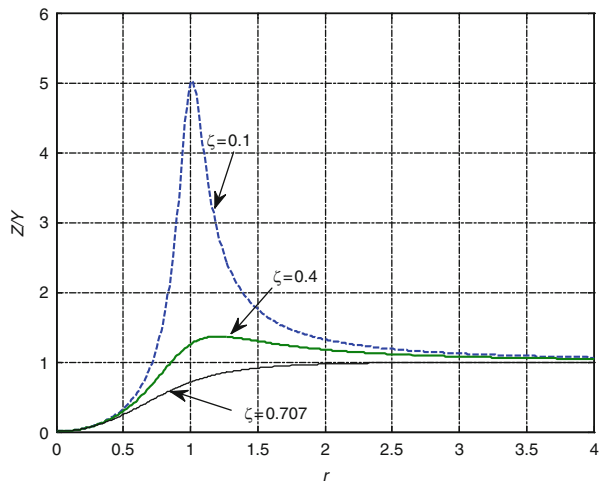


**Fig. 2.17** A plot for the relative deflection of a structure excited from the base normalized to the amplitude input

Now consider the quantity  $z(t)\omega_n^2$ . From Eq. (2.45), it can be written as

$$z(t)\omega_n^2 = \frac{\Omega_b^2 Y \cos(\Omega_b t - \theta)}{\sqrt{(1 - r^2)^2 + (2\zeta r)^2}}. \tag{2.47}$$

Recall that  $\ddot{y} = -\Omega_b^2 Y \cos(\Omega_b t - \theta)$ , hence according to Eq. (2.47)

$$z(t)\omega_n^2 = \frac{-\ddot{y}}{\sqrt{(1 - r^2)^2 + (2\zeta r)^2}}. \tag{2.48}$$

Note that as  $r \rightarrow 0$ ;  $\frac{1}{\sqrt{(1-r^2)^2+(2\zeta r)^2}} \rightarrow 1$ . Hence, from Eq. (2.48), in this case the relative displacement is proportional to the base acceleration as  $|z(t)\omega_n^2| = |\ddot{y}|$ .

The previous observation represents the basic principle of **accelerometers**. By measuring the relative deflection of the structure inside the accelerometer through a transduction mechanism, for instance electrostatic or piezoelectric, the acceleration of the base is determined. This is provided again that  $r$  is sufficiently small. To further quantify this condition, we plot in Fig. 2.18 the ratio  $\frac{1}{\sqrt{(1-r^2)^2+(2\zeta r)^2}}$  for small range of  $r$  for various values of  $\zeta$ . As noted from the figure, this ratio remains equal to unity for the largest range of  $r$  when  $\zeta = 0.707$ . Hence, by tuning the damping of the accelerometer to be near this damping ratio, the maximum operating range of the device is achieved. It is agreed on that for accurate measurements,  $r$  must be less than 0.2. This means that the natural frequency of the accelerometer should be at least five times higher than the measured frequency. This implies that the mass of the

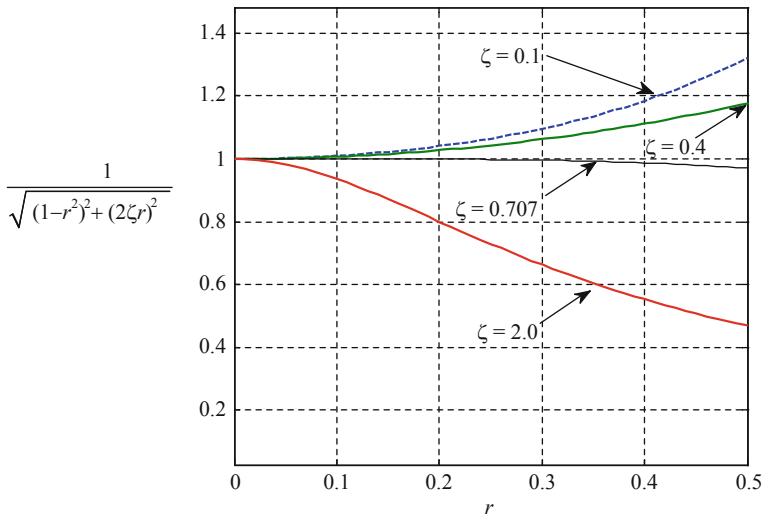


**Fig. 2.18** A plot for the coefficient of  $\ddot{y}$  versus the normalized frequency for various values of damping ratios

accelerometer should be small enough to satisfy this condition. It turns out that this requirement in addition to the requirement of high damping near critical are easily satisfied via the MEMS technology. Through MEMS, the size of the accelerometer is made very small making the useful range of the accelerometer very large. Also, through the naturally existing squeeze-film damping, achieving critical damping is neither difficult nor costly in the micro scale. Therefore, no wonder that MEMS accelerometers were among the first and most successful MEMS devices that made it to commercialization.

## 2.6 Response of SDOF Systems to Arbitrary Excitation

Sections 2.3 and 2.4 deal with forced vibration, in which a system is constantly being excited by a harmonic force. In many situations, systems can be excited by nonharmonic and even nonperiodic forces, which may last for limited duration of time. A common example in the macro and micro applications is the mechanical shock force, which is induced on a structure when dropped on the ground. This force can take the shape of a pulse, for example triangle or half-sine, of limited duration, corresponding to the time of contact between the body and the ground. As a result of such a force, a flexible structure can get excited and undergo oscillatory motion over several cycles before the motion dies out due to damping.

In this section, we discuss the response of SDOF systems subjected to an arbitrary excitation based on the convolution integral approach without going into derivations details. For an undamped system, such as that of Fig. 2.2a, subjected to a force  $F(t)$  of an arbitrary profile, Fig. 2.19, the response of the system can be expressed as

$$x(t) = \frac{1}{m\omega_n} \int_0^t F(\tau) \sin[\omega_n(t - \tau)] d\tau. \quad (2.49)$$

For an underdamped system, such as that of Fig. 2.4a, subjected to  $F(t)$ , the response of the system is calculated by

$$x(t) = \frac{1}{m\omega_d} \int_0^t F(\tau) e^{-\zeta\omega_n(t-\tau)} \sin[\omega_d(t - \tau)] d\tau. \quad (2.50)$$

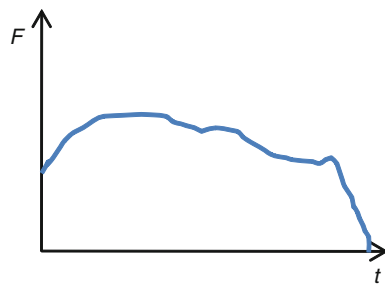


**Fig. 2.19** An example of a force of arbitrary profile

Equations (2.49) and (2.50) predict the total response of the system due to the applied force assuming trivial initial conditions. For other initial conditions, Eqs. (2.49) and (2.50) represent only the particular solution for the equation of motion due to the force. The total response will then be composed of Eq. (2.49) or Eq. (2.50) plus the homogenous solution (corresponding to zero force). From relating the total solution to the initial conditions, the constants of integration of the homogenous solution are determined. This is further clarified in Example 2.7. Calculating the integrals in Eqs. (2.49) and (2.50) can be difficult analytically. Hence, numerical approaches, such as the trapezoidal method, can be used, which are found readily in software, such as Mathematica [12] and Matlab [13].

**Example 2.6:** Calculate the response of an undamped SDOF system, Fig. 2.2a, when subjected to a suddenly applied constant force  $F_0$  (step force), Fig. 2.20. Assume trivial initial conditions for the system.

**Solution:** The equation of motion for this system is written as

$$m\ddot{x} + kx = F(t) \quad (2.51)$$

where  $F(t)$  is an arbitrary force. Hence, applying Eq. (2.49) yields

$$x(t) = \frac{1}{m\omega_n} \int_0^t F_0 \sin[\omega_n(t - \tau)] d\tau = \frac{-F_0}{m\omega_n} \frac{\cos[\omega_n(t - \tau)]}{-\omega_n} \Big|_0^t \quad (2.52)$$

$$\Rightarrow x(t) = \frac{F_0}{k} [1 - \cos(\omega_n t)]. \quad (2.53)$$

**Example 2.7:** Calculate the response of an undamped SDOF system, Fig. 2.21, dropped to the ground from a distance  $h$ . This problem models the drop test used in the industry to test the survivability of portable devices and electronics including MEMS.

**Solution:** At the instant the system touches the ground, the spring will be pushed upward from its base. Also, at that moment, the whole system will be under the influence of the gravity acceleration  $-g$ , where the negative sign indicates that the acceleration is in a direction opposite to  $x$  (downward). This is similar to the base

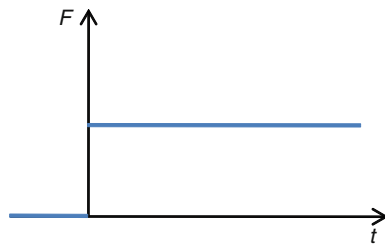


**Fig. 2.20** A step force applied at time zero

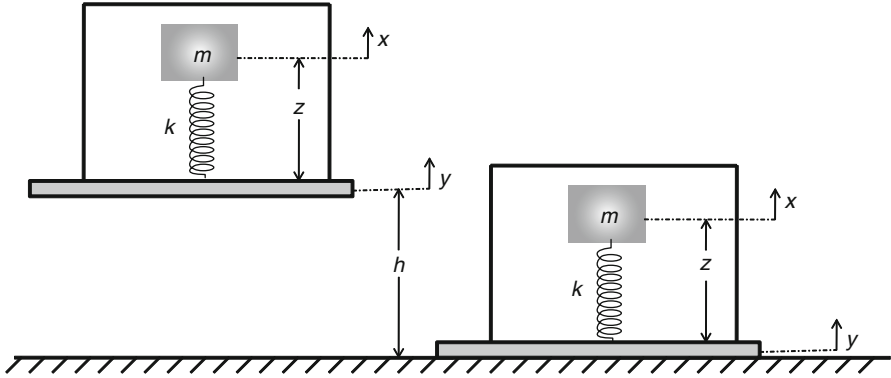


Fig. 2.21 A model for a drop test of a packaged device of Example 2.7

excitation problem of Sect. 2.4, except that the force here is not harmonic but arbitrary (constant). From Eq. (2.42), the equation of motion for this system is expressed as

$$m\ddot{z} + kz = -m\ddot{y} = mg = F_0 \quad (2.54)$$

which is similar to the case of Example 2.6 except that here the system is not initially at rest. The initial velocity of the system at the time of contact  $v_0$  can be found from equating the potential energy  $mgh$  to the kinetic energy  $mv_0^2/2$ , which gives

$$v_0 = \sqrt{2gh}. \quad (2.55)$$

The total solution for Eq. (2.54) is composed of a particular solution given by Eq. (2.53) and a homogeneous solution given by Eq. (2.9), that is

$$x(t) = \frac{F_0}{k}[1 - \cos(\omega_n t)] + A \sin(\omega_n t + \phi). \quad (2.56)$$

Substituting  $F_0 = mg$ ,  $k = m\omega_n^2$ , using the initial conditions  $x_0 = 0$  and Eq. (2.55), and solving for  $A$  and  $\phi$  yield

$$x(t) = \frac{g}{\omega_n^2}[1 - \cos(\omega_n t)] + \frac{\sqrt{2gh}}{\omega_n} \sin(\omega_n t). \quad (2.57)$$

To find the instantaneous acceleration for the mass, Eq. (2.57) is differentiated twice with respect to time:

$$\ddot{x}(t) = g \cos(\omega_n t) - \omega_n \sqrt{2gh} \sin(\omega_n t). \quad (2.58)$$

Alternatively, Eq. (2.58) can be written as

$$\ddot{x}(t) = g \sqrt{1 + \frac{2h\omega_n^2}{g}} \sin \left[ \omega_n t + \tan^{-1} \left( \frac{-g}{\omega_n v_0} \right) \right]. \quad (2.59)$$

Hence, the maximum acceleration magnitude is given by

$$|\ddot{x}_{\max}| = g \sqrt{1 + \frac{2h\omega_n^2}{g}}. \quad (2.60)$$

We note from Eq. (2.60) that the maximum induced acceleration increases with the height of drop  $h$  and the natural frequency of the system.

**Example 2.8:** A more accurate model for the shock force induced from the impact of a system with the ground is achieved by modeling it as a pulse force or acceleration of finite duration. As an example, consider a rectangular pulse force of amplitude  $F_0$  and duration  $t_1$ , Fig. 2.22. Calculate the response of the undamped system of Fig. 2.2a to this force pulse assuming trivial initial conditions.

**Solution:** The force of Fig. 2.22 can be expressed as

$$F(t) = \begin{cases} F_0 & 0 \leq t \leq t_1 \\ 0 & t_1 \leq t \end{cases}. \quad (2.61)$$

Since the force is split into two parts, the response of the system is also split into two parts. For the first time period,  $0 \leq t \leq t_1$  the scenario looks exactly like the case of Example 2.6 (the system is always under the influence of  $F_0$  during this time interval). Hence, the response of the system in this interval is given by Eq. (2.53). For the second time interval,  $t_1 \leq t$ , the convolution integral, Eq. (2.49), is applied as

$$x(t) = \frac{1}{m\omega_n} \int_0^{t_1} F_0 \sin[\omega_n(t - \tau)] d\tau + \frac{1}{m\omega_n} \int_{t_1}^t 0 \times \sin[\omega_n(t - \tau)] d\tau \quad (2.62)$$

where the integral has been split into two parts to account for the discontinuity of the force over time, as expressed in Eq. (2.61). Calculating the above integrals yields

$$x(t) = \frac{F_0}{k} \{ \cos[\omega_n(t - t_1)] - \cos(\omega_n t) \}. \quad (2.63)$$

In summary, the response of the system is given by

$$x(t) = \begin{cases} \frac{F_0}{k} [1 - \cos(\omega_n t)] & 0 \leq t \leq t_1 \\ \frac{F_0}{k} \{ \cos[\omega_n(t - t_1)] - \cos(\omega_n t) \} & t_1 \leq t \end{cases}. \quad (2.64)$$

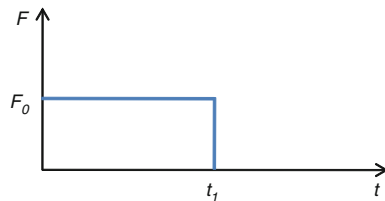


**Fig. 2.22** A rectangular pulse that can be used to model shock forces

## 2.7 Vibrations of Two-Degree-of-Freedom Systems

This section presents an introduction to an important topic, which is the vibration of multi-DOF systems. This topic is too big to be covered in a single section or even in a single chapter. Here, we attempt to go over the basic elements of this subject, which have direct applications in MEMS. For more in-depth coverage of this topic, the reader is referred to any of these books [1–5].

We focus next on systems that need two independent coordinates to describe their motions. These are called 2-DOF systems. Figure 2.23 shows examples of such. Note that for each system, two independent coordinates are needed to fully describe the motion, which can be translational or rotational coordinates. Examples of such systems in MEMS include filters made of two coupled oscillators, gyroscopes, directional microphones, and devices placed over flexible printed-circuit boards.

### 2.7.1 Undamped Free Vibration and Eigenvalue Problem

As with SDOF systems, we start by analyzing the free vibration of 2-DOF systems. To illustrate the procedure, we consider as an example the system shown in Fig. 2.24. The first step in the analysis is to write the equations of motion for the system. Typically, this can be done using Lagrange's or energy approaches for complicated multi-DOF systems. These are outside the scope of this book. Hence, whenever it is possible, we

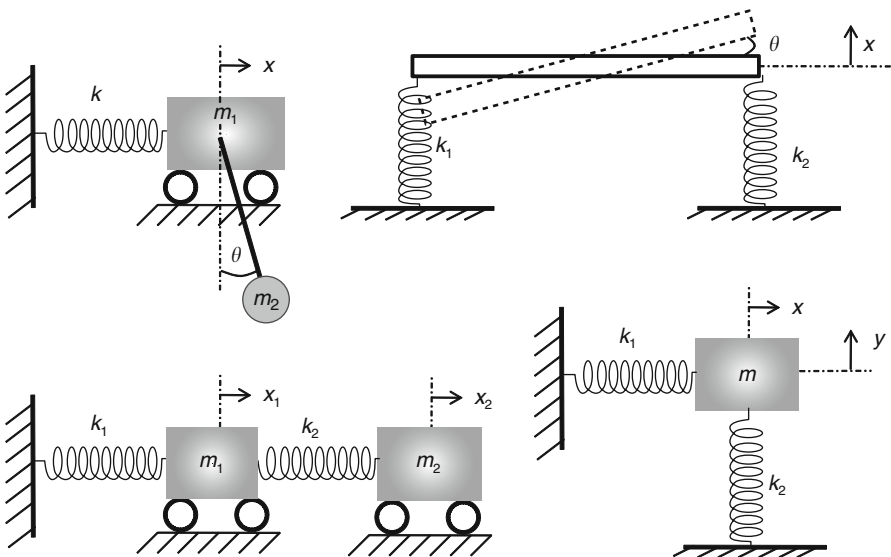


Fig. 2.23 Examples of 2-DOF systems

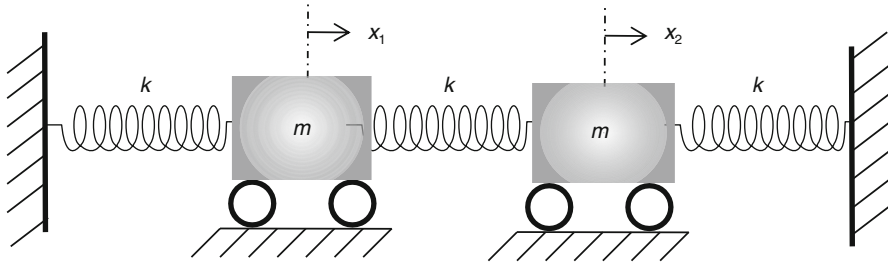


Fig. 2.24 A 2-DOF system

will use the Newtonian or force-diagram approach. In this approach, each mass is separated from the system and all the forces acting on it in the considered directions of motion are considered. In this example, the masses move in the horizontal direction, hence the horizontal forces are analyzed. Assuming each mass is displaced to the positive direction to the right, the resistance forces will be as depicted in Fig. 2.25.

Based on Fig. 2.25, the equation of motion of each mass is written as

$$-kx_1 + k(x_2 - x_1) = m\ddot{x}_1 \Rightarrow m\ddot{x}_1 + 2kx_1 - kx_2 = 0 \tag{2.65}$$

$$-kx_2 - k(x_2 - x_1) = m\ddot{x}_2 \Rightarrow m\ddot{x}_2 - kx_1 + 2kx_2 = 0. \tag{2.66}$$

Equations (2.65) and (2.66) are two coupled linear second-order differential equations. The fact that they are coupled means that we cannot solve one equation independently from the other; both need to be solved simultaneously. For convenience, we cast them in a matrix format as

$$\underbrace{\begin{bmatrix} m & 0 \\ 0 & m \end{bmatrix}}_{[m]} \begin{Bmatrix} \ddot{x}_1 \\ \ddot{x}_2 \end{Bmatrix} + \underbrace{\begin{bmatrix} 2k & -k \\ -k & 2k \end{bmatrix}}_{[k]} \begin{Bmatrix} x_1 \\ x_2 \end{Bmatrix} = \begin{Bmatrix} 0 \\ 0 \end{Bmatrix} \tag{2.67}$$

where  $[m]$  is called the mass matrix and  $[k]$  is called the stiffness matrix. To solve the system of Eq. (2.67), we assume

$$\begin{aligned} x_1 &= X_1 e^{i\omega t} \\ x_2 &= X_2 e^{i\omega t} \end{aligned} \tag{2.68}$$

where  $i$  is the imaginary root. This is equivalent to assuming that each mass vibrates in harmony with the other; hence, they vibrate with the same frequency  $\omega$  but with

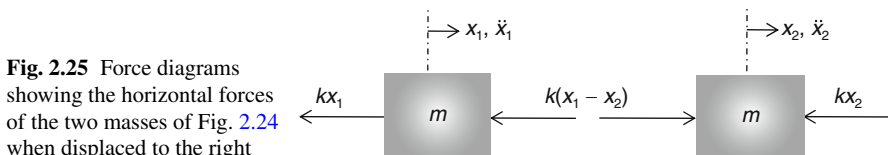


Fig. 2.25 Force diagrams showing the horizontal forces of the two masses of Fig. 2.24 when displaced to the right

different amplitudes,  $X_1$  and  $X_2$  for mass one and two, respectively. Substituting Eq. (2.68) into Eq. (2.67), dividing by  $e^{i\omega t}$ , and regrouping the coefficients yield

$$[[k] - \omega^2[m]] \{X\} \Rightarrow \begin{bmatrix} 2k - \omega^2 m & -k \\ -k & 2k - \omega^2 m \end{bmatrix} \begin{Bmatrix} X_1 \\ X_2 \end{Bmatrix} = \begin{Bmatrix} 0 \\ 0 \end{Bmatrix}. \quad (2.69)$$

Equation (2.69) is a homogenous algebraic system of equations in  $X_1$  and  $X_2$ . Multiplying both sides by the inverse of the matrix  $[[k] - \omega^2[m]]$  yields simply that  $X_1$  and  $X_2$  are zeros (trivial solution) meaning no vibrations. Our only hope for not ending with this result is to reconsider the matrix  $[[k] - \omega^2[m]]$  and assume that this matrix is non-invertible (singular matrix). Mathematically this means its determinant must be equal to zero.

To summarize, to obtain nontrivial solutions, we need to solve Eq. (2.69) as an eigenvalue problem by first setting the determinant of  $[[k] - \omega^2[m]]$  equal to zero. This yields the following quadratic (characteristic) equation in  $\omega^2$ :

$$(2k - \omega^2 m)^2 - k^2 = 0. \quad (2.70)$$

Solving Eq. (2.70) for  $\omega^2$  yields the so-called eigenvalues

$$\omega^2 = \frac{k}{m}; \quad \omega^2 = \frac{3k}{m}. \quad (2.71)$$

Taking the square roots yields

$$\begin{aligned} \omega_1 &= \sqrt{\frac{k}{m}}; & \omega_2 &= \sqrt{\frac{3k}{m}}; \\ \omega_3 &= -\sqrt{\frac{k}{m}}; & \omega_4 &= -\sqrt{\frac{3k}{m}}. \end{aligned} \quad (2.72)$$

The positive roots,  $\omega_1$  and  $\omega_2$ , are the natural frequencies of the system. This is a major feature characterizing 2-DOF systems compared to SDOF systems; they have two natural frequencies instead of one. To proceed, we need to solve for the ratio of  $X_1$  with respect to  $X_2$ , the so-called eigenvectors or modeshapes, for each eigenvalue. For this, each value of  $\omega^2$  in Eq. (2.71) is substituted into Eq. (2.69). Then, one of the two resulting equations in  $X_1$  and  $X_2$  is solved to determine the ratio  $X_1/X_2$ . The second equation is dependent on the first, hence one needs to use only one of the two equations. Substituting  $\omega^2 = k/m$  and adopting the first equation (first row) gives

$$\left(2k - \frac{k}{m} \times m\right) X_1 - kX_2 = 0 \Rightarrow \frac{X_1}{X_2} = 1. \quad (2.73)$$

From Eq. (2.73), we say that the first eigenvector  $v_1$  corresponding to the natural frequency  $\omega_1$  is equal  $v_1 = \begin{Bmatrix} 1 \\ 1 \end{Bmatrix}$ . This means that for some initial conditions, if the system happens to vibrate in  $\omega_1$  only, then the ratio of the displacement of the first mass to the second mass is equal 1. In another word, if the first mass is displaced a

distance one unit to the right, the second mass will also be displaced a one unit to the right. This is the meaning of the eigenvector or modeshape.

Similarly, substituting  $\omega^2 = 3k/m$  and adopting the first equation give

$$\left(2k - \frac{3k}{m} \times m\right) X_1 - kX_2 = 0 \Rightarrow \frac{X_1}{X_2} = -1. \quad (2.74)$$

From Eq. (2.74), the second eigenvector  $v_2$  corresponding to the natural frequency  $\omega_2$  is equal to  $v_2 = \begin{Bmatrix} 1 \\ -1 \end{Bmatrix}$ . This means that for some initial conditions, if the system happens to vibrate in  $\omega_2$  only, then the ratio of the displacement of the first mass to the second mass is equal  $-1$ . In another word, if the first mass is displaced a distance one unit to the right, the second mass will also be displaced a one unit to the left. We should mention here that an eigenvector is arbitrary within a constant. So if we multiply it by any number  $\alpha$ , it remains the same eigenvector. What really matters is the ratio between the individual elements of the eigenvector and not their absolute values.

After finding the natural frequencies and modeshapes, the free response of each mass can be expressed in term of those as

$$\begin{aligned} \begin{Bmatrix} x_1(t) \\ x_2(t) \end{Bmatrix} &= B_1 \begin{Bmatrix} 1 \\ 1 \end{Bmatrix} e^{i\omega_1 t} + B_2 \begin{Bmatrix} 1 \\ 1 \end{Bmatrix} e^{-i\omega_1 t} \\ &+ B_3 \begin{Bmatrix} 1 \\ -1 \end{Bmatrix} e^{i\omega_2 t} + B_4 \begin{Bmatrix} 1 \\ -1 \end{Bmatrix} e^{-i\omega_2 t} \end{aligned} \quad (2.75)$$

where  $B_1$ – $B_4$  are constants of integration, which are determined from the initial conditions of the system. Equivalently, Eq. (2.75) can be rewritten as

$$\begin{Bmatrix} x_1(t) \\ x_2(t) \end{Bmatrix} = A_1 \begin{Bmatrix} 1 \\ 1 \end{Bmatrix} \sin(\omega_1 t + \phi_1) + A_2 \begin{Bmatrix} 1 \\ -1 \end{Bmatrix} \sin(\omega_2 t + \phi_2) \quad (2.76)$$

where also the constants  $A_1$ ,  $A_2$ ,  $\phi_1$ , and  $\phi_2$  are determined from the initial conditions of the system, for example Eq. (2.77) below:

$$x_1(0) = x_{10}; \quad x_2(0) = x_{20}; \quad \dot{x}_1(0) = v_{10}; \quad \dot{x}_2(0) = v_{20}. \quad (2.77)$$

Substituting Eq. (2.77) in either Eq. (2.75) or Eq. (2.76), four algebraic equations are obtained for the constant of integrations, which are then solved simultaneously.

### 2.7.2 Modal Analysis

Modal analysis is the key procedure to study the damped and forced vibrations of multi-DOF systems. In this procedure, the coupled system of differential equations governing the vibration of a multi-DOF system is decoupled into independent SDOF

systems, which can be solved using the information in Sects. 2.2–2.6. To illustrate the procedure, consider the below undamped multi-DOF system subjected to the force vector  $\{F(t)\}$ :

$$[m]\{\ddot{x}\} + [k]\{x\} = \{F(t)\}. \quad (2.78)$$

In Eq. (2.78), the matrices  $[m]$  and  $[k]$  are generally not diagonal, and hence the equations of motion are coupled. To decouple them, a transformation is used that transforms the physical coordinates  $\{x\}$  into “modal coordinates”  $\{y\}$  as

$$\{x\} = [s]\{y\} \quad (2.79)$$

where the transformation matrix  $[s]$  is composed of the normalized eigenvectors of the system  $v_j^n$ , calculated as in Sect. 2.7.1, being put in columns as

$$[s] = [v_1^n v_2^n v_3^n \dots]. \quad (2.80)$$

The normalization of the eigenvectors is done as below

$$\{v_j^n\}^T [m] \{v_j^n\} = 1 \quad (2.81)$$

where the superscript  $T$  denotes transpose.

Next, we substitute Eq. (2.79) into Eq. (2.78) and multiply the outcome by  $[s]^T$

$$[s]^T [m] [s] \{\ddot{y}\} + [s]^T [k] [s] \{y\} = [s]^T \{F(t)\}. \quad (2.82)$$

It turns out that the following facts are true for Eq. (2.82) and the transformation matrix  $[s]$ :

- $[s]^{-1} = [s]^T [m]$ .
- $[s]^T [m] [s] = [I]$ , where  $[I]$  is the identity matrix.
- $[s]^T [k] [s] = [\Lambda]$ , where  $[\Lambda]$  is a diagonal matrix composed of the eigenvalues of the system, that is  $[\Lambda] = \begin{bmatrix} \omega_1^2 & & \\ & \omega_2^2 & \\ & & \dots \end{bmatrix}$ .

Thus, our objective of getting diagonal matrices is achieved. The individual SDOF equations due to the transformation are written as

$$\begin{aligned} \ddot{y}_1 + \omega_1^2 y_1 &= f_1 \\ \ddot{y}_2 + \omega_2^2 y_2 &= f_2 \\ \vdots & \quad \quad \quad \vdots \end{aligned} \quad (2.83)$$

where  $f_1, f_2 \dots$  are the modal forces. For a 2-DOF system, they are given by

$$\begin{Bmatrix} f_1(t) \\ f_2(t) \end{Bmatrix} = [s]^T \begin{Bmatrix} F_1(t) \\ F_2(t) \end{Bmatrix}. \quad (2.84)$$



The transformation matrix is written as

$$s = \frac{1}{\sqrt{2m}} \begin{bmatrix} 1 & 1 \\ 1 & -1 \end{bmatrix}. \quad (\text{d})$$

The second step is to calculate the modal forces according to Eq. (2.84):

$$\begin{Bmatrix} f_1(t) \\ f_2(t) \end{Bmatrix} = [s]^T \begin{Bmatrix} \cos(\Omega t) \\ 0 \end{Bmatrix} = \frac{1}{\sqrt{2m}} \begin{Bmatrix} \cos(\Omega t) \\ \cos(\Omega t) \end{Bmatrix}. \quad (\text{e})$$

Next, the modal equations are written according to Eq. (2.86). Substituting the values of  $k$ ,  $\zeta_1$ ,  $\zeta_2$ , and  $m$  and recalling the values of  $\omega_j^2$  from Sect. 2.7.1 yield

$$\begin{aligned} \ddot{y}_1 + 2\zeta_1\omega_1\dot{y}_1 + \omega_1^2y_1 = f_1 &\Rightarrow \ddot{y}_1 + \dot{y}_1 + 100y_1 = \frac{\cos(\Omega t)}{\sqrt{2}} \\ \ddot{y}_2 + 2\zeta_2\omega_2\dot{y}_2 + \omega_2^2y_2 = f_2 &\Rightarrow \ddot{y}_2 + 0.7\dot{y}_2 + 300y_2 = \frac{\cos(\Omega t)}{\sqrt{2}}. \end{aligned} \quad (\text{f})$$

Equations (f) are solved according to Eqs. (2.32)–(2.34) as below:

$$\begin{aligned} y_1(t) &= Y_1 \cos(\Omega t - \theta_1) \\ y_2(t) &= Y_2 \cos(\Omega t - \theta_2) \end{aligned} \quad (\text{g})$$

where

$$\begin{aligned} Y_1 &= \frac{1/\sqrt{2}}{\sqrt{(100 - \Omega^2)^2 + (\Omega)^2}} \\ Y_2 &= \frac{1/\sqrt{2}}{\sqrt{(300 - \Omega^2)^2 + (.7\Omega)^2}} \end{aligned} \quad (\text{h})$$

$$\begin{aligned} \theta_1 &= \tan^{-1} \left( \frac{\Omega}{100 - \Omega^2} \right) \\ \theta_2 &= \tan^{-1} \left( \frac{0.7\Omega}{300 - \Omega^2} \right). \end{aligned} \quad (\text{i})$$

Transforming back to the physical coordinates using Eq. (2.79) yields

$$\begin{Bmatrix} x_1 \\ x_2 \end{Bmatrix} = \frac{1}{\sqrt{2}} \begin{bmatrix} 1 & 1 \\ 1 & -1 \end{bmatrix} \begin{Bmatrix} Y_1 \cos(\Omega t - \theta_1) \\ Y_2 \cos(\Omega t - \theta_2) \end{Bmatrix}. \quad (\text{j})$$

Substituting for the values of  $Y_1$  and  $Y_2$  gives the final expressions for  $x_1$  and  $x_2$ :

$$x_1(t) = \frac{\cos(\Omega t - \theta_1)}{2\sqrt{(100 - \Omega^2)^2 + (\Omega)^2}} + \frac{\cos(\Omega t - \theta_2)}{2\sqrt{(300 - \Omega^2)^2 + (.7\Omega)^2}} \quad (\text{k})$$

$$x_2(t) = \frac{\cos(\Omega t - \theta_1)}{2\sqrt{(100 - \Omega^2)^2 + (\Omega)^2}} - \frac{\cos(\Omega t - \theta_2)}{2\sqrt{(300 - \Omega^2)^2 + (.7\Omega)^2}}. \quad (\text{l})$$

Figure 2.26 shows the response of each mass in time.

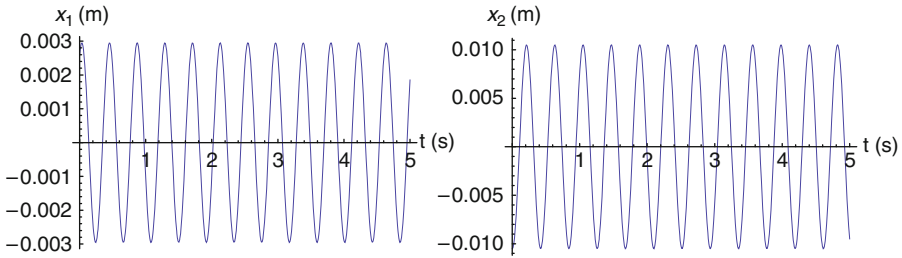


**Fig. 2.26** The time–history response of the first and second mass of Example 2.9

### 2.7.3 Resonances in 2-DOF Systems

In a 2-DOF system, there are two resonance frequencies (and in an  $n$ -DOF systems, there are  $n$  resonance frequencies). They occur when the system is excited near one of its natural frequencies. For example, for the system described in Sect. 2.7.1 and in Example 2.9, we should expect resonances near  $\Omega = 10$  rad/s and 17.3 rad/s. The next example illustrates this further.

**Example 2.10:** Plot the frequency–response curves of the system of Example 2.9 and show its resonances.

**Solution:** The responses are given in Eqs. (k) and (l) in Example 2.9. To plot the frequency–response curves, we need to rewrite the response expression in terms of amplitude and phase. For simplicity, we let

$$A_1 = \frac{1}{2\sqrt{(100 - \Omega^2)^2 + (\Omega)^2}}; \quad A_2 = \frac{1}{2\sqrt{(300 - \Omega^2)^2 + (.7\Omega)^2}}. \quad (a)$$

Then, using trigonometric identities of the cosine of the sum of two angles, it can be shown that

$$x_1(t) = X_1 \sin[\Omega t + \Phi_1]; \quad x_2(t) = X_2 \sin[\Omega t + \Phi_2]; \quad (b)$$

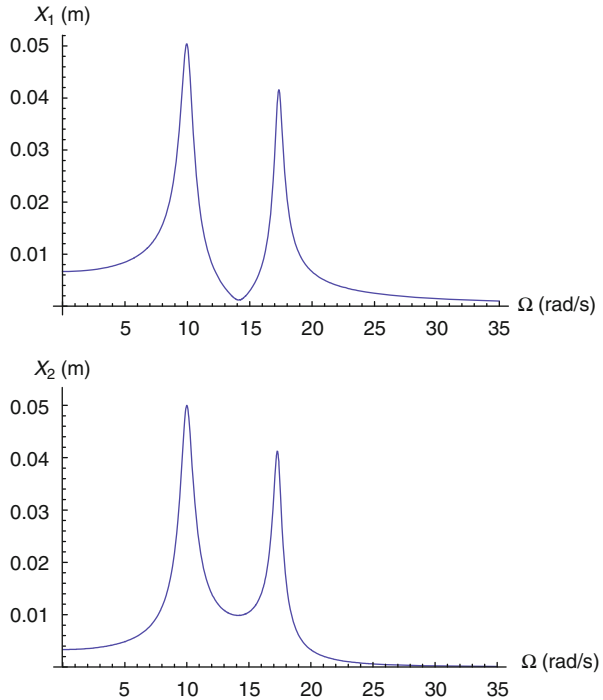
where

$$X_{1,2} = \sqrt{A_1^2 + A_2^2 \pm 2A_1 A_2 \cos(\theta_1 - \theta_2)} \quad (c)$$

$$\Phi_{1,2} = \tan^{-1} \left( \frac{A_1 \sin(\theta_1) \pm A_2 \sin(\theta_2)}{A_1 \cos(\theta_1) \pm A_2 \cos(\theta_2)} \right). \quad (d)$$

Figure 2.27 shows the frequency–response curve obtained from Eqs. (a) and (c). It is clear that both masses exhibit resonant behaviors near the natural frequencies of the system at  $\Omega = 10$  rad/s and  $\Omega = 17.3$  rad/s.

**Fig. 2.27** Frequency–response curves of the first and second mass of Example 2.9



## 2.8 Numerical Integration

In the previous sections, we discussed analytical techniques to solve for the response of systems to initial conditions and to forcing, harmonic and arbitrary. The analytical results and expressions can reveal valuable information about the response without even plugging numbers. However, in many situations, such as in the presence of nonlinearities, analytical solutions may not be available or possible. Even if the analytical solutions are available, it is recommended to check the validity of these using numerical techniques and software. Numerical techniques, such as the Runge-Kutta method, can be used to integrate the equation of motion in time, and hence solve the equation of motion numerically.

This section gives an introduction to the numerical integration techniques using the software Mathematica [12] and Matlab [13]. These will be used and referred to more frequently in the subsequent chapters. In Matlab, there are many ordinary-differential equations (ODE) solvers, such as *ode45* and *ode23*. To use those, the user needs to write a main program, an *m* file, to input the various parameters of the problem and to process the obtained solutions, and a subprogram, another *m* file, which contains the equations of motion written in state-space representation. In Mathematica, one can use the command *NDSolve*, which does not require casting the equations in state-space format. Without further introduction, we demonstrate the use of these in the following examples.

**Example 2.11:** Write Matlab and Mathematica codes to simulate the response of a spring–mass–damper system to a generic excitation force using numerical integration. Then, solve Example 2.2 and compare to the analytical results.

**Solution:**

1. **Matlab:** To solve this problem in Matlab, the equation of motion needs to be rewritten in state-space representation, which is to transform the equation of motion into a system of first-order differential equations in time. Consider below the general SDOF equation normalized by the mass:

$$\ddot{x} + \frac{c}{m}\dot{x} + \frac{k}{m}x = \frac{F(t)}{m}. \quad (\text{a})$$

To write Eq. (a) in a state-space form, we let  $x_1 = x$  and  $x_2 = \dot{x}$ . Then Eq. (a) becomes:

$$\begin{aligned} \dot{x}_1 &= x_2; \\ \dot{x}_2 &= -\frac{c}{m}x_2 - \frac{k}{m}x_1 + \frac{F(t)}{m}. \end{aligned} \quad (\text{b})$$

The below Matlab code is used to find the response of Example 2.2. The code yields the same results as shown in Fig. 2.8.

- (a) The main Program (the *m* file is called *main1*).

```
%This program solves the response of a SDOF system to
% a generic force.
%Below is the solution for example 2.2 using
%numerical time integration.
clear all;clc;close all
global m k c F %This is to make those parameters
%identified in both the main program and the
%subprogram.
m=1;
k=100;
c=1;

%Tint is the time interval for the time integration
%(start and end).
tend=12;
Tint=[0 tend];

%Below are the initial conditions of the system.
x0=0;
v0=0.01;
Int=[x0 v0];

%This the main time integration command. It calls
%a subroutine that we build in a separate m-file,
%called eq1. The output will be two vectors: t:
%refers to the time vector and x1: refers to the
%displacement vector.
[t,x1]=ode45('eq1',Tint,Int);
```

```
%Below is the plot of the solution in mm.
plot(t,x1(:,1)*1000);xlabel('t(s)');ylabel('x (mm)');
```

- (b) The subroutine program (the  $m$  file is called *eq1*).

```
%This is the subprogram or subroutine where the
%equations of motion are entered.
%The subroutine must be named as it was called in
%the main program (in this case it must be
%named 'eq1'
function dxdt(eq1(t,x)
global m k c
F=0; %This is the forcing in the system.
%The equations of motion below are written in
%state-space form.
dxdt=[x(2);
      -k/m*x(1)-c/m*x(2)+F/m];
```

2. **Mathematica:** Below are the command lines to solve this problem (note that in Mathematica multiplication is expressed using a space between the various variables and numbers):

```
tend=12;
x0=.0;
v0=0.01;
m=1;
k=100;
c=1;
solution(Flatten[NDSolve[{x''[t]+c/m x'[t]+k/m
x[t]==0,x[0]==x0,x'[0]==v0},x[t], {t,tend},MaxSteps->10^9]];
Plot[Evaluate[(x[t])*1000 /.solution],
{t,0,tend},PlotRange->All,AxesLabel->{"t (s)","x (mm)"}]
```

**Example 2.12:** Solve Example 2.6 using numerical integration assuming  $F_0 = 10$  N,  $m = 1$  kg, and  $k = 100$  N/m and compare to the analytical results.

**Solution:**  $\omega_n = \sqrt{k/m} = 10$  rad/s. Hence, the analytical solution Eq. (2.53) becomes

$$x(t) = 0.1[1 - \cos(10t)]. \quad (\text{a})$$

1. **Matlab:** We use similar  $m$ -files of the previous example with slight modifications for this problem input. Figure 2.28 shows the results. Below are the used code:

- (a) The main program (the  $m$  file is called *main2*).

```
%Below is the solution for example 2.12 using numerical
time integration.
clear all;clc;close all
global m k c
m=1;
k=100;
c=0;
```

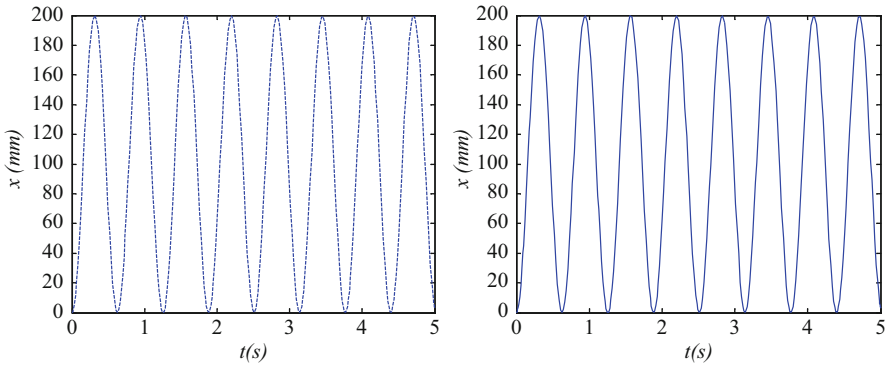


**Fig. 2.28** A comparison of the time history response of Example 2.12 obtained analytically (*left*) to that obtained using time integration (*right*)

```
tend=5;
Tint=[0 tend];

x0=0;
v0=0.01;
Int=[x0 v0];
[t,x1]=ode45('eq2',Tint,Int);

%Below is the plot of the numerical solution in mm.
plot(t,x1(:,1)*1000);xlabel('t (s)');ylabel('x (mm)');

%Below is the plot of the analytical solution in mm.
Xanalyt=0.1*(1-cos(10*t));
figure; plot(t,Xanalyt*1000,'--');
xlabel('t (s)');ylabel('x (mm)');
```

- (b) The subroutine program (the *m* file is called *eq2*).

```
%This is the subprogram named 'eq2'
%function dxdt(eq2(t,x)
global m k c
F=10*stepfun(t,0); %This defines a unit-step function
%multiplied by 10.
%The equations of motion below are written in state-
%space presentation.
dxdt=[x(2);
      -k/m*x(1)-c/m*x(2)+F/m];
```

2. **Mathematica:** The same command lines of Example 2.11 can be used after adjusting the damping and the forcing as below:

```
solution=Flatten[NDSolve[{x''[t]+c/m x'[t]+k/m
x[t]==10 UnitStep[t], x[0]==x0, x'[0]==v0}, x[t],
{t,tend},MaxSteps->10^9]];
```

## 2.9 MEMS Band-Pass Filters

Perhaps one of the earliest researched MEMS devices since the beginning of the technology is the MEMS band pass filter. Since the mid-sixties, Nathanson and coworkers at Westinghouse demonstrated in a series of papers the attractive features of electrostatically actuated microbeams, called resonant gate transistors, such as their high-quality factors, their excellent thermal properties, and their desirable band-pass filter characteristics [14, 15]. This is in addition to the more significant advantage of their ability to interface with integrated electronics at the board level (on-chip integration), which is essential for miniaturization. This cannot be achieved with conventional off-chip bulky filters. Nathanson et al. [14, 15] have noticed that the distinctive large response of these microbeams when driven near their resonance frequencies qualify them as distinguished band pass filters, which pass signals at frequencies within a certain range near resonance and attenuate signals at frequencies outside this range. Nowadays, MEMS filters are commonly used in communication systems, such as wireless and cellular applications. They come in various designs and shapes, and not necessarily based on coupled vibrating systems.

In addition to realizing a band-pass filter from the vibration of a single microstructure near resonance, Nathanson et al. [15] have proposed the use of coupled multiple filters to improve their performance. This is achieved by mechanically connecting more than one vibrating microstructure of close resonant frequencies to each other through a weak mechanical coupler, for example Fig. 2.29. The bandwidth of the filter is then determined by the stiffness of the mechanical coupler. This has the effect of widening the bandwidth of the filter and improving the roll-off from the pass-band to the stop-band (making the transition from the resonance regime to nonresonant regime steeper and faster). In recent years, many studies have been presented on MEMS filters to increase their operating frequency and improve their overall performance, see for instance [16–18].

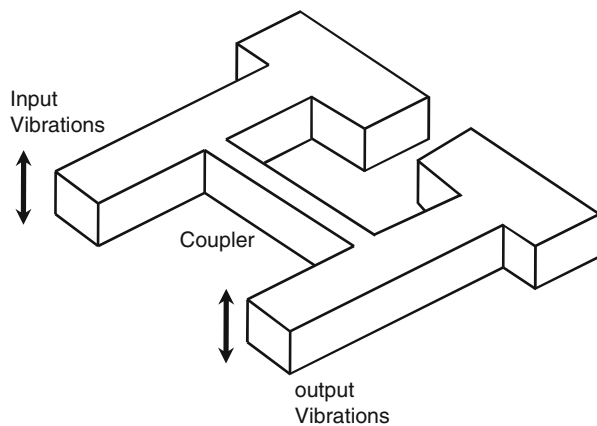


**Fig. 2.29** Schematic of one of the possible configurations of a MEMS band-pass filter

**Fig. 2.30** The response of a band-pass filter showing some of its key parameters

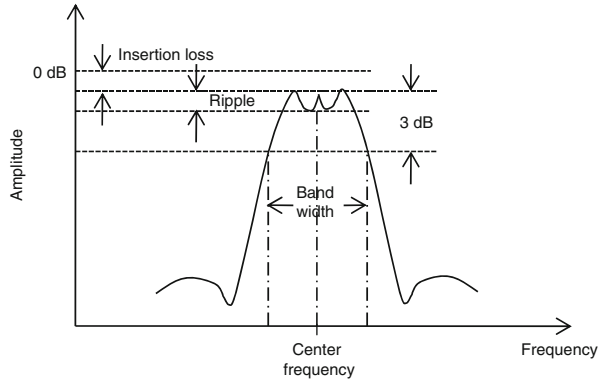


Figure 2.30 shows an example of the response of a band-pass filter explaining some of its main characteristics. A good band pass filter in general has a high-quality factor, low insertion loss (insertion loss is the ratio of output to input signals of the filter; it measures the reduction of the signal power as it passes the filter), flat pass band (minimum ripples), and sharp or rapid roll off from the pass-band to stop band.

**Example 2.13:** Consider the 2-DOF model of a band-pass filter of Fig. 2.31. Assume  $m = 0.1 \text{ g}$ ,  $k = 1 \text{ N/m}$ ,  $c = 0.6 \text{ g/s}$  and  $F = 0.1 \text{ }\mu\text{N}$ . Calculate the response of the second unforced mass (output) for (a)  $\delta k = 0.06 \text{ N/m}$  and (b)  $\delta k = 0.1 \text{ N/m}$ .

**Solution:** The equation of motion of the system can be written as

$$m\ddot{x}_1 + c\dot{x}_1 + (k + \delta k)x_1 - \delta kx_2 = F \cos \Omega t \tag{a}$$

$$m\ddot{x}_2 + c\dot{x}_2 + (k + \delta k)x_2 - \delta kx_1 = 0. \tag{b}$$

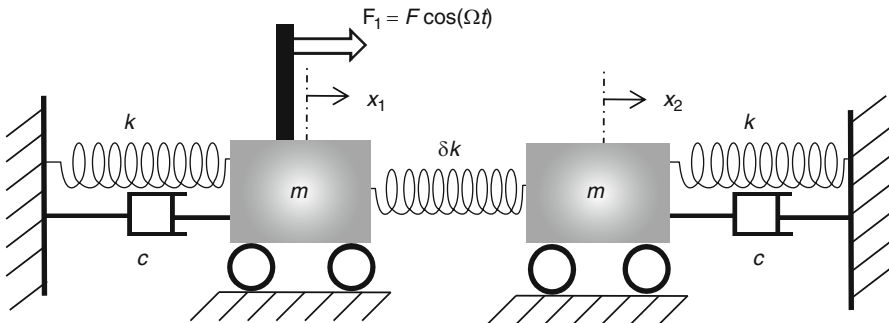


**Fig. 2.31** A model of a two coupled microstructures acting as a band-pass filter

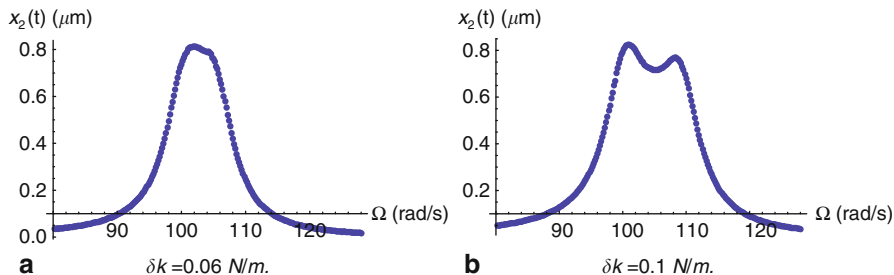


**Fig. 2.32** The response of the unforced mass of Fig. 2.31 showing a band-pass filter characteristic

Using modal analysis as in Sect. 2.7.1, it is found that the natural frequencies of the system are expressed as

$$\omega_1 = \sqrt{\frac{k}{m}}; \quad \omega_2 = \sqrt{\frac{(k + 2\delta k)}{m}}. \quad (c)$$

Hence, one can see that the larger the value of  $\delta k$  is the larger the separation between the two frequencies is, which means a wider bandwidth. Equations (a) and (b) can be solved using modal analysis, similar to Sect. 2.7.2, or can be integrated numerically directly, as in Sect. 2.8. Here we choose to use the second method as an exercise toward learning the procedure for the more complicated nonlinear problems. In this method, a for-loop is built to run over several values of excitation frequencies. At each excitation frequency, a numerical integration of the equations of motion is carried out over a sufficient period of time that guarantees that the system reaches steady-state response (one can check this visually by plotting the time history response for a single excitation frequency). Then, the maximum value of the response over the last oscillation period of the time response is calculated. This represents a single point on the frequency response at the current excitation frequency of the for-loop. Repeating this for several values of the excitation frequency yields the complete frequency-response curve. The results are depicted in Fig. 2.32. Note that the bandwidth has increased with the increase of  $\delta k$ .

## Problems

1. For the SDOF system of Fig. 2.4a, given  $m = 1$  kg,  $k = 100$  N/m, and assuming the system has trivial initial conditions, calculate and plot the response of the system for the following cases:
  - (a)  $c = 0$  kg/s.
  - (b)  $c = 2$  kg/s.
  - (c)  $c = 20$  kg/s.
  - (d)  $c = 40$  kg/s.
  - (e) Verify your results in (a)–(d) using numerical integration for the equation of motion, as in Sect. 2.8, using Matlab or Mathematica.

2. For the SDOF system of Fig. 2.9a, given  $m = 10$  kg,  $k = 4000$  N/m, and  $c = 200$  kg/s, calculate
  - (a) The undamped natural frequency.
  - (b) The damped natural frequency.
  - (c) The resonance frequency.
  - (d) The peak frequency (where the amplitude of the response is maximum).
  - (e) The steady-state amplitude of the response at resonance.
  - (f) The peak steady-state amplitude (at the peak frequency).
  - (g) Verify your results in (e) and (f) using numerical integration for the equation of motion, as in Sect. 2.8, using Matlab or Mathematica.
3. Assume the device of Fig. 2.16a, with  $m = 0.01$  kg,  $k = 100$  N/m, and  $c = 0.2$  kg/s, is subjected to a harmonic base excitation of amplitude 10 mm. Calculate the maximum steady-state relative deflection of the device with respect to the base for:
  - (a) Excitation frequency equals 10 Hz.
  - (b) Excitation frequency equals 30 Hz.
  - (c) Excitation frequency at resonance.
4. Solve Example 2.8 assuming a triangular pulse force, Fig. 2.33, instead of the rectangular pulse of Fig. 2.22. (Hint: you may want to use Mathematica to carry out the convolution integrals).
5. For the 2-DOF system of Fig. 2.34, write the equations of motion for the system and then calculate
  - (a) The natural frequencies of the system.
  - (b) The corresponding mode shapes.
  - (c) The transformation matrix  $S$ .
  - (d) The amplitude of the steady-state response of each mass for  $\Omega = 10$  rad/s assuming  $m = 1$  kg and  $k = 100$  N/m.
  - (e) Verify your results in (d) using numerical integration for the equation of motion, as in Sect. 2.8, using Matlab or Mathematica.
  - (f) The values of  $\Omega$  that will cause resonance for the system.
6. Consider the band-pass filter of Example 2.13. Investigate the variation of the damping coefficient  $c$  on the performance of the filter.

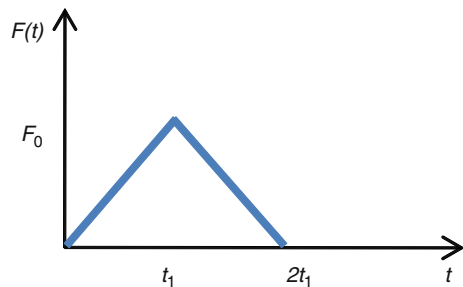


**Fig. 2.33** Schematic of a triangular pulse for Problem 4

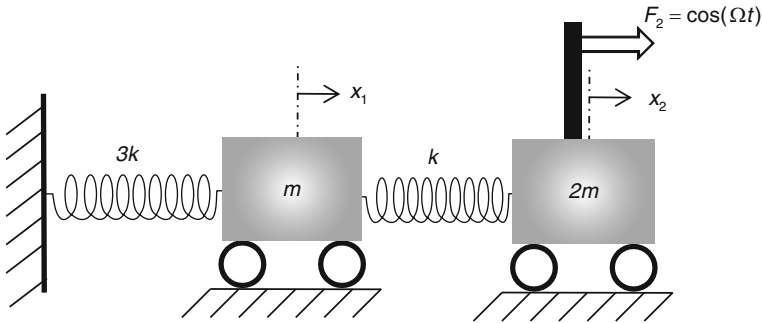


Fig. 2.34 The two-DOF system of Problem 5

## References

- [1] Inman D J (2008) Engineering vibration. Third Edition, Prentice Hall, New Jersey
- [2] Thomson W T, Dahleh M D (1998) Theory of vibration with applications. Fifth Edition, Prentice Hall, New Jersey
- [3] Rao S S (2004) Mechanical vibrations. Fourth Edition, Prentice Hall, New Jersey
- [4] Meirovitch L (2001) Fundamentals of vibrations. Fourth Edition, McGraw Hill, New York
- [5] Balachandran B, Magrab E (2009) Vibrations. Second Edition, Cengage Learning, Toronto
- [6] Yazdi N, Ayazi F, Najafi K (1998) Micromachined inertial sensors. Proceedings of the IEEE, 86(8):1640–1659
- [7] Liu K, Zhang W, Chen Wn, Li K, Dai F, Cui F, Wu X, Ma G, Xiao Q (2009) The development of micro-gyroscope technology. Journal of Micromechanics and Microengineering, 19:113001(29pp)
- [8] Acar C, Shkel A (2009) MEMS vibratory gyroscopes. Springer, New York
- [9] L. Meirovitch (1970) Methods of analytical dynamics. McGraw-Hill, New York
- [10] Roundy S, Wright P K, Rabaey J (2003) A study of low level vibrations as a power source for wireless sensor nodes. Computer Communications, 26:1131–1144
- [11] Stephen N G (2006) On energy harvesting from ambient vibration. Journal of Sound and Vibration, 293:409–25
- [12] www.wolfram.com (Wolfram Research, Inc.; Champaign, IL)
- [13] www.mathworks.com (Mathworks; Natick, MA)
- [14] Nathanson H C, Wickstrom R A (1965) A resonant-gate silicon surface transistor with high-Q band-pass properties. Applied physics letters, 7(4):84–86
- [15] Nathanson H C, Newell W E, Wickstorm R A, Davis J R (1967) The resonant gate transistor. IEEE Transaction on Electron Devices, ED-14(3):117–133
- [16] Bannon F D, Clark J R, Nguyen C T-C (2000) High-Q HF microelectromechanical filters. IEEE Journal of Solid-State Circuits, 35:512–526
- [17] Lin L, Nguyen C T-C, Howe R T, Pisano A P (1992) Microelectromechanical filters for signal processing. In Proceeding IEEE Micro Electro Mechanical Systems MEMS 1992, Trarvumunde, Germany, pp. 226–231
- [18] Varadan V M, Vinoy K J, Jose K A (2003) RF MEMS and their applications, Wiley, New York